NUMERICAL STUDY OF UPSTREAM AND DOWNSTREAM REGIONS OF ONE DIMENSIONAL DETONATION WAVE IN A DUSTY GAS MEDIUM

by

SHUBHADEEP BANIK

A THESIS

Presented to the Faculty of the Graduate School of the

MISSOURI UNIVERSITY OF SCIENCE AND TECHNOLOGY

In Partial Fulfillment of the Requirements for the Degree

MASTER OF SCIENCE IN MECHANICAL ENGINEERING

2015

Approved by

Dr. Kakkattukuzhy M. Isaac, Advisor
Dr. James A. Drallmeier
Dr. Joshua Rovey

PUBLICATION THESIS OPTION

This thesis has been prepared in the style utilized by the Journal of Propulsion and Power. Pages 4-42 will be submitted for publication in that journal. Appendices A and B have been added for purposes normal to thesis writing.

ABSTRACT

In detonative combustion very high temperatures are attained by the burned gases. As a result, a large amount of thermal energy is produced during the combustion process. This heat can affect the state of the unburned fuel through radiation of heat from the burned gases. In this study a one-dimensional model was deemed appropriate to gain insight into the fundamental structure of the detonation wave. In this model, the detonation wave divides the fluid stream into an upstream region, consisting of fuel and oxidant, and a downstream region, consisting of burned gases. A set of computer programs, some developed during the present work and others developed by other investigators, were used in combination. These codes, when used in conjunction with an appropriate chemical reaction mechanism, can work for most gaseous fuel/oxidant mixtures. Ethane-air, methane-air, syngas-air and acetylene-oxygen mixtures, seeded with solid carbon particles, were used. Variation in flow properties were obtained for both the unburned and burned regions. The temperature levels observed in the burned region supports the previous statement regarding high thermal energy generation. The flame structure of the detonation wave region was studied. To study the effect of radiative heating in the unburned upstream region, appropriate emissivity and absorptivity models from literature were used. Carbon particles have a significant role in the upstream side, and as the results reveal, they have a relatively higher heat absorbing capacity than the gaseous components. A study of the amount of burned gas considered represented by the path length in evaluating the amount of heat radiated was also done to understand its effect on the upstream side.

ACKNOWLEDGEMENTS

I would like to express my sincere gratitude to my advisor Dr. Kakkattukuzhy M. Isaac for providing me an opportunity to work on a challenging research problem. His mentorship was invaluable to me in the endeavor to accomplish the assigned work. Additionally, courses taught by him provided a sound knowledge of the fundamentals of thermal and fluid sciences which were applied in this study.

I would also like to thank Dr. James A. Drallmeier and Dr. Joshua Rovey who agreed to be on my graduate committee and gave a critique of my thesis. I am grateful to the Department of Mechanical and Aerospace Engineering for providing Graduate Teaching Assistantship, which gave me opportunities to assist different faculty in their courses. Guidance from Mrs. Vicki Hudgins and other staff members of the Office of Graduate Studies in preparing the thesis in an appropriate format is gratefully acknowledged.

Finally, I thank my family for their encouragement in pursuing graduate studies and their affection.

TABLE OF CONTENTS

Page

LIST OF ILLUSTRATIONS

Figure Page

PAPER

LIST OF TABLES

INTRODUCTION

Detonation is defined as a shock wave sustained by the energy released by combustion, which in turn, is initiated by the shock-wave compression and the resulting high temperatures [1]. If a long tube with an open end and a closed end is considered, and a fuel is ignited at the closed end, then a flame would initiate at the closed end. The burned gas, trapped between the flame and the closed end, tries to expand and consequently accelerates the flame. This acceleration results in the development of a shock wave. So, in a coordinate frame w.r.t. a laboratory, a detonation wave moves through the fluid. For analyses, the detonation wave is considered stationary and the fluid moves through it with different velocities in the upstream and downstream regions of the wave. The coordinate frame is considered to be fixed to the wave. In detonations, the downstream flow has sonic velocity. Across a detonation wave velocity decreases, whereas, pressure, temperature and density increase.

The results of the present study can help in the development of propulsion applications, such as a pulse detonation engine (PDE), and for studying the effects of explosions in general. In explosions, damage is caused due to the presence of a supersonic wave front and attainment of extremely high pressures, in contrast to subsonic combustion.

In this thesis, radiative heating of the upstream region of a detonation wave is studied. The heat is generated in the downstream region due to very high temperatures attained during combustion. Four fuel-oxidizer mixtures, seeded with solid particles, were selected for different case studies. The manuscript presented here focuses on the

results of three fuel-air mixtures seeded with solid carbon particles. Results from the study of a fuel-oxygen mixture are presented separately in the appendix. The methodology used in case of acetylene-oxygen is a bit different than the fuel-air mixtures.

REFERENCES

[1] S. R. Turns, An Introduction to Combustion, McGraw-Hill, 2000.

[2] R. J. Santoro and S.-Y. Lee, "PULSE DETONATION ENGINES: PROGRESS AND CHALLENGES," *International Journal of Energetic Materials and Chemical Propulsion,* vol. 6, no. 4, pp. 441-461, 2007.

[3] K. Kailasanath, "A REVIEW OF PDE RESEARCH - PERFORMANCE ESTIMATES," in *39th AIAA Aerospace Sciences Meeting & Exhibit*, Reno, NV, 2001.

[4] G. Roy, S. Frolov, A. Borisov and D. Netzer, "Pulse detonation propulsion: challenges, current status,and future perspective," *Progress in Energy and Combustion Science,* vol. 30, no. 6, pp. 545–672, 2004.

[5] J. Griner and K. Isaac, "Induction Time and Detonation Wave Structure of Acetylene, Ethylene and JP-10," in *Proceedings of the 2002 Technical Meeting of the Central States Section of the Combustion Institute* , 2002.

[6] A. Kazakov and Frenklach, "http://www.me.berkeley.edu/drm/," Dec 2014.

[7] J. Zhao, "CJWave-Performs detailed analysis of flow across a Chapman-Jouguet wave and combustion downstream.," Missouri University of Science and Technology, Mechanical and Aerospace Engineering Department, Rolla, 1991.

[8] http://elearning.cerfacs.fr/combustion/tools/adiabaticflametemperature/index.php. "eLearning at CERFACS", Dec 2014.

[9] A. Coppalle and P. Vervisch, "The Total Emissivities of High-Temperature Flames," *Combustion and Flame,* no. 49, pp. 101-108, 1983.

PAPER

Radiative Heating of Dusty Gas Fuel-Air Mixtures in One Dimensional Detonation

Shubhadeep Banik[1] and Kakkattukuzhy M. Isaac[2]

Missouri S&T, Rolla, MO, 65409

ABSTRACT

High flame temperatures, reached in detonative combustion, lead to a large amount of heat generation. This can heat fresh fuel through radiation. The objective of the present study is to numerically investigate the effect of radiative heating of a gas-solid fuel mixture. To model the problem, a one dimensional detonation process is considered where the detonation wave divides the fluid stream into an upstream region, consisting of unburned reactants, and a downstream region, containing combustion products. Multiple fuel-air mixtures, with varying proportions of carbon particles, were considered. Chemical species composition and variation in flow properties – temperature, pressure, Mach number and density – were obtained for the downstream region. The upstream region is assumed to be a constant area duct with frictionless flow. A finite difference method is used to obtain heat flux and

---

[1] Graduate Assistant, Mechanical & Aerospace Eng., 400 W. 13th St., Rolla, MO 65409, AIAA Student member.
[2] Professor & Associate Chair, Mechanical & Aerospace Engineering, 400 W. 13th St., Rolla, MO 65409, Associate fellow.

static temperature variations in the upstream region. The distance from the shock wave front to the upstream location, where 99.99 percent of the heat radiated from the combustion products is absorbed, is considered as the absorbing distance. Results show that increasing the volume fraction of solid phase in the mixture by a factor of 10 led to decrement in absorbing distance by a factor of 2 to 4.

NOMENCLATURE

a = absorptivity, cm^2/mol

a = radius of solid particles, m

b = optical path length, cm

c = concentration, mol/cm^3

c = local speed of sound, m/s

c_p = specific heat capacity at constant pressure, J/(kg-K)

c_s = specific heat capacity of solid particles, J/(kg-K)

c_v = specific heat capacity at constant volume, J/(kg-K)

f_v, α = volume fraction

h = specific enthalpy, J/kg

I = Intensity of transmitted laser signal, mV

I_0 = Intensity of total laser signal, mV

i = index in x direction

L = path length of gas in the downstream region, m

M = Mach number

m = complex index of refraction

mw = molecular weight, kg/mol

P, p = pressure, Pa

Q = efficiency factor

q = heat, W

q_f = heat flux, W/m^2

R = specific gas constant, J/ (kg-K)

R_u = universal gas constant, J/ (mol-K)

T = temperature, K

u = velocity, m/s

x = horizontal direction

Δx = step size in x direction

Y = species mass fraction

α = absorptance

γ = specific heat ratio

ε = emissivity

κ_λ = absorption coefficient for small particles, (1/m)

$\kappa_{p\eta}$ = pressure absorption coefficient, 1/ (m-Pa)

λ = wavelength, m

σ = Stefan-Boltzmann constant, W/ (m^2-K^4)

ρ = density, kg/m^3

χ = mole fraction

ω = species production rate, kg/ (m^3/s)

$\Im$ = imaginary part

Subscript

abs = absorption

C = continuous phase

D = disperse phase

ext = extinction

f = flame

i = index

ig = ignition point

mix = gaseous mixture

sca = scattering

T = total

0 = stagnation

1 = entrance location

2 = exit location

1. INTRODUCTION

Detonations can release an immense amount of energy at a rapid rate. In the last 60 years, research has been done to harness this rapid energy release in propulsion applications [1]. Pulse detonation engine (PDE) is one such application, which is still in the developmental stage. In detonation, parameters such as ignition delay, deflagration-to-detonation transition (DDT), and wave structure need to be studied to make PDE fully functional [2]. Griner and Isaac [3] determined induction times for multiple fuels. In one

case, they report large amounts of heat release from the combustion products. The present study focuses on the effect of the radiative heating on the fresh fuel-air mixture seeded with solid particles. In some recent studies [4, 5], detonation initiation and DDT are also shown to occur primarily as a result of radiative heating of unburned fuel mixtures.

Multi-dimensional numerical simulations of detonations can be performed depending on the parameters that need to be studied. Such studies on detonation wave structure have been compiled by Oran [6] and Nikolaev et al. [7]. To study geometrically more complex problems, instead of using multidimensional models, Nikolaev et al. [7] suggested using quasi-one dimensional models. Shepherd [8] provided a comprehensive overview of numerical simulations of detonations, including one-dimensional models, with simplified, and detailed chemical reaction kinetics. A one-dimensional model to study unsteady detonations was proposed by Bdzil and Davis [9]. Research done in the field of detonations in gas-particle mixtures can be found, for example, in [10, 11]. A one-dimensional model can attain the goals of the present study of a steady detonation wave, as will be discussed in the later sections.

Heaslet and Baldwin [12] used an analytical/numerical approach and showed how thermal radiation affects the structure of a shock wave. Velocity and temperature profiles obtained in their study for strong and weak shocks have a discontinuity, or an imbedded adiabatic shock. Zel'dovich [13] obtained similar discontinuities in velocity, density and temperature profiles in his shock wave studies. Work of other researchers who numerically studied the interaction of radiative heat with a shock wave can be found in [14-17]. Drake [18] obtained temperature profiles in the upstream and downstream regions of optically thick radiative shocks, which are found in astrophysical systems.

Buckley [19] numerically studied effects of radiative heat flux in shock waves in gas-particle flows and graphically showed the extent to which those effects are felt in the upstream region. The aforementioned studies do not involve combustion or chemical reaction. In the domain of detonation, Raghunandan investigated [20, 21] radiative heating of fresh ethane-air mixture, without solid particles, by combustion products. The formulations were based on static temperature. The basic equation used in the current study (Eq. (30)) is formulated using stagnation temperature instead of static temperature. The stagnation temperature-based model is more accurate than the formulation based on static temperature. Additionally, in comparison to Raghunandan's study, here an ideal gas assumption for gaseous mixtures based on upstream conditions was considered. It helped in determining molecular weight and specific heat of gases in gas-particle mixtures in a relatively easier way. In this way, characteristics of fuels other than those discussed here, can also be studied in a convenient way. In Raghunandan's work, molecular weights and specific heats were derived from CHEMKIN [32]. The procedure is quite involved. A parameter "absorbing distance", discussed later in the results section, is the indication of the heat absorbing capacity of different gas-particle mixtures. In this study it is calculated in terms of the amount of radiative heat coming from the downstream region. In the study by Raghunandan, the same was done based on a comparison of the calculated static temperature and the inlet static temperature.

2. PROBLEM DESCRIPTION AND MATHEMATICAL FORMULATION

A one-dimensional (1D) detonation model, as proposed by Isaac and Scott [2], is shown in Fig. 1. Fuel-air mixture flows along the positive 'x' direction. The detonation

wave is considered to be fixed in space, with the coordinate system attached to it. Upstream of the wave, the flow is supersonic. Immediately after the wave, the flow becomes subsonic, and gradually increases to sonic velocity. At certain location in the downstream region, the mixture gets auto-ignited. In Fig. 1, the distance from the detonation wave to the point of ignition is the ignition distance. The corresponding flow time, referred to as convective time, would represent ignition delay.

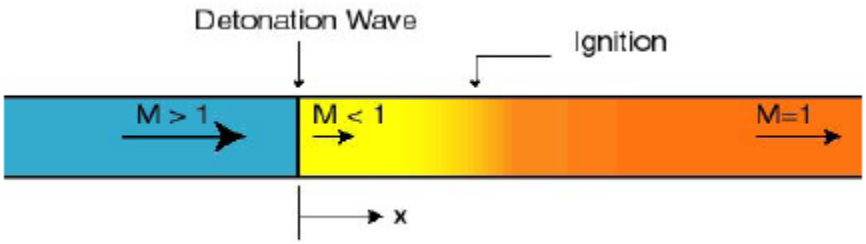

Fig.1 A one dimensional detonation process (blue zone has the lowest temperature, followed by yellow, and orange zone which has the highest temperature).

In Fig. 1, the upstream region ($x < 0$) consists of the unburned reactants, whereas the region downstream of the ignition point ($x > x_{ig}$) contains the combustion products. Heat generated in the downstream region is radiated to the upstream region, as shown in Fig. 2. The amount of heat generated depends on the temperature, pressure and composition of the combustion products; these are discussed in the following sections.

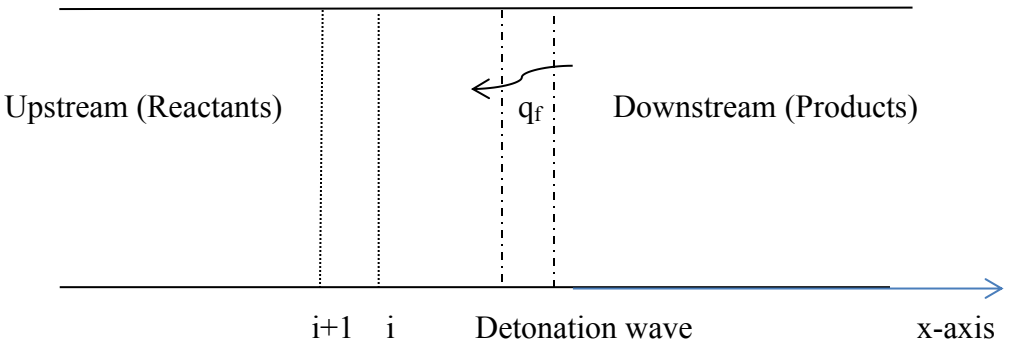

Fig. 2 Radiative heating of upstream region.

Flow in the downstream region can be described by Eqs. (1-4), that are the steady state equations for conservation of mass, momentum, energy and chemical species, respectively.

$$\frac{d(\rho u)}{dx} = 0 \tag{1}$$

$$\frac{dp}{dx} + \rho u \frac{du}{dx} = 0 \tag{2}$$

$$\frac{dh}{dx} + u \frac{du}{dx} = 0 \tag{3}$$

$$\frac{dY_i}{dx} = \frac{\omega_i}{\rho u} \tag{4}$$

To study the effect of radiative heating of the upstream region, the model of a frictionless constant-area flow with stagnation temperature change (Rayleigh flow) is chosen [22]. The stagnation temperature change is determined by the following equation.

$$T_{02} = T_{01} + \frac{q}{c_p} \tag{5}$$

We assume the ideal gas model for the upstream gas mixture since the upstream temperature is not high enough (~300K) for real gas effects to be significant. Under this assumption, the other flow properties in the upstream region are computed using Eqs. (6-9).

$$\frac{T_0}{T} = 1 + \frac{\gamma - 1}{2} M^2 \tag{6}$$

$$\frac{T_{02}}{T_{01}} = \left[\frac{1 + \gamma M_1^2}{1 + \gamma M_2^2} \left(\frac{M_2}{M_1} \right) \right]^2 \left(\frac{1 + \frac{\gamma - 1}{2} M_2^2}{1 + \frac{\gamma - 1}{2} M_1^2} \right) \tag{7}$$

$$\frac{P_0}{P} = (1 + \frac{\gamma - 1}{2} M^2)^{\frac{\gamma}{\gamma - 1}} \tag{8}$$

$$\frac{T}{T_1} = (\frac{P}{P_1} \frac{M}{M_1})^2 \tag{9}$$

The upstream flow is seeded with solid particles to form a two-phase mixture, or a "dusty gas." The effect of adding particles will be discussed in the case studies presented in later sections. The two-phase mixture consists of a continuous phase, denoted by C, and a disperse phase, denoted by D. A loading parameter ξ is defined as follows.

$$\xi = \frac{\rho_D \alpha_D}{\rho_C \alpha_C} \tag{10}$$

A homogeneous flow model, in which there is no relative motion or temperature difference between the different phases, was considered. Mass exchange between the two components was also neglected. Consequently, ξ was treated as a constant for the flow. For practical purposes, it was assumed that volume fraction of continuous phase $\alpha_C \approx 1$. With this approximation, the two phase gas mixture can be treated as a single phase fluid or an "effective gas" [23]. Now, the equation of state of the effective gas can be written as

$$p = \rho R T \tag{11}$$

where R is the specific gas constant of the effective gas. The following relations apply for the properties of the effective gas.

$$\rho = \rho_C (1 + \xi) \tag{12}$$

$$R = \frac{R_C}{1 + \xi} \tag{13}$$

$$c_p = \frac{c_{pC} + \xi c_{sD}}{1 + \xi} \tag{14}$$

$$\gamma = \frac{c_{pC} + \xi c_{sD}}{c_{vC} + \xi c_{sD}} \tag{15}$$

$$c = c_C \left[\frac{1 + \frac{\xi c_{sD}}{c_{pC}}}{\left(1 + \frac{\xi c_{sD}}{c_{vC}}\right)(1+\xi)} \right]^{\frac{1}{2}} \quad (16)$$

c_C is the isentropic speed of sound in the continuous phase and is given as follows.

$$c_c = \sqrt{\gamma_c R_c T} \quad (17)$$

3. RADIATIVE PROPERTIES

Emissive characteristics of the combustion products are required to determine the amount of heat radiated into the upstream region. The radiated heat is gradually absorbed in the upstream region by the reactant mixture. To account for this, absorptive properties of the mixtures are needed.

A. Emissivity model

The radiative heat from products of combustion is calculated as follows.

$$q_f = \varepsilon \sigma T_f^4 \quad (18)$$

Emissivity of the products of combustion is computed based on the work of Coppalle et al. [24], which provides the coefficients α_i, β_i and K_i. It is as follows.

$$\varepsilon_T = \sum_{i=1}^{4} (\alpha_i + \beta_i T)[1 - e^{-K_i pL}] \tag{19}$$

where, p is the sum of the partial pressures of CO_2 and water vapor. Here only CO_2 and water vapor are considered because almost the entire radiated heat comes from these two species [24].

B. Absorptivity model

The present study involves three fuel-air mixtures which are seeded with dust particles. The individual absorptive characteristics of fuel and dust particles are as follows.

1. Ethane

Absorptivity of ethane, used in the study, has been obtained from the work of Olson et al. [25]. Absorptivity is defined as follows.

$$a = \frac{\log_{10}\left(\frac{I_o}{I}\right)}{bc} \tag{20}$$

For ethane, absorptivity is given by the following expression.

$$a = (4.78 \pm 0.03) \times 10^4 - 10.01T - 0.0017T^2 \tag{21}$$

c is obtained by using Eq. (22).

$$c_i = \frac{\chi_i P}{R_u T} \tag{22}$$

2. Methane

Absorption coefficient of methane, obtained from the work of Wakatsuki [26], is shown in Eq. (23). Values of the coefficients of the polynomial expression used in this study can be found in Table 4 in the Appendix.

$$\kappa_{p\eta,i} = a_0 + a_1 T_i + a_2 T_i^2 + a_3 T_i^3 + a_4 T_i^4 \tag{23}$$

Both absorptivity of ethane and absorption coefficient of methane are parameters that provide the absorptive properties of ethane and methane, respectively. However, they are defined in different ways, as shown in Eqs.(21,23), and have different units. To make a comparison, absorptances of ethane and methane were compared (see section 4) and a relation between absorption coefficient and absorptivity, which would work for both fuels, was obtained and is shown in Eq. (24).

$$a = \frac{\kappa_{p\eta,i} P}{c} \tag{24}$$

In Eq. (24), same standard of units should be used.

3. Syngas

The composition of syngas used in the study, as shown in Table 5 in the Appendix, consists of methane as the only hydrocarbon fuel. So, the absorption coefficient shown in Eq. (23) is used for syngas.

4. Dust particles

The dust particles are solid carbon particles having 0.027 μm diameter. Previously an experimental study by Lanzo et al. involved investigation of heat transfer to a gas

seeded with carbon particles of the aforementioned dimension [27]. These are much smaller than the wavelength of infrared radiation occurring in combustion applications. A size parameter of the particles is defined as follows.

$$x = \frac{2\pi a}{\lambda} \tag{25}$$

For such fine particles, x<<1. Therefore, Rayleigh scattering criteria can be used to determine absorption and scattering properties of the carbon particles. The efficiency factors are given as follows.

$$Q_{sca} = \frac{8}{3}\left|\frac{m^2-1}{m^2+2}\right|^2 x^4 \tag{26}$$

$$Q_{abs} = -4\Im\left\{\frac{m^2-1}{m^2+2}\right\}x \tag{27}$$

where $m = n - ik$. As $x^4 << x$,

$$Q_{ext} = Q_{sca} + Q_{abs} \approx Q_{abs} \tag{28}$$

Therefore, scattering may be neglected as compared to absorption. Absorption coefficient for small particles is given as follows [28].

$$\kappa_\lambda = \frac{36\pi nk}{(n^2 - k^2 + 2)^2 + 4n^2k^2} \frac{f_v}{\lambda} \tag{29}$$

The absorption coefficient of the carbon particles should be added to that of the fuel-air mixture to obtain the total absorption coefficient of the dusty gas [29].

4. METHODOLOGY

To investigate radiative heat transfer occurring in the detonation process, different numerical approaches are used for the two domains, consisting of the downstream and the upstream regions, respectively.

A. Downstream region

In the downstream region, the fine carbon particles are not expected to contribute to the combustion process as their number density is very small, and the chemical energy released due to their burning would be negligible compared to that released by the combustion of the fuel gas. Combustion of the carbon particles would not significantly affect heat release and species mass fractions. The initial conditions of all the fuel-air mixtures were: P = 0.1 atm, T = 300K, M = 7.4. Using a step size of 0.005 cm, Eqs. (1-4) were solved using the FORTRAN program CJwave [30]. The step size has to be small because Eq. 4 involves large reaction rates, which cause stiffness in the equations. To deal with stiffness, an ordinary differential equation solver package LSODE [31] was used. CJwave calls CHEMKIN [32] subroutines to obtain the thermodynamic properties and their derivatives, species production rates and their derivatives, and sensitivity parameters. The user provides an appropriate chemical reaction mechanism to

CHEMKIN as input. The DRM 19 mechanism, a subset of the GRI-MECH 1.2 mechanism [33], was used in this work for all the fuels. DRM 19 has 21 species and 84 reactions.

B. Upstream region

In the upstream region, radiative heating of the dusty gas is considered. A FORTRAN subroutine named 'upstream' was used for the upstream calculations. It uses Eqs. (5-9) to determine the flow properties and Eqs. (10-17) to account for the carbon particles. The upstream region is divided into finite computational cells. A computational cell is shown in Fig. 3.

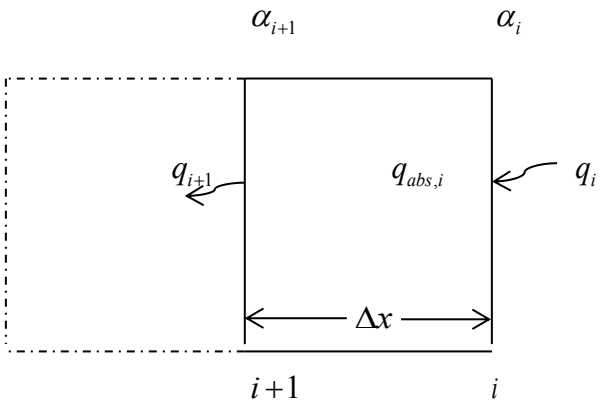

Fig. 3 A computational cell.

An explicit finite-difference formulation of Eq. (5) to calculate the stagnation temperature is as follows.

$$T_{0_{i+1}} = T_{0_i} - \frac{\alpha_i q_{f,i}}{\rho_i u_i c_{p,mix}} \tag{30}$$

In Eq. (30), α_i represents the absorbed part of the incoming radiative heat. For ethane-air mixture, absorptance is computed as the product of absorptivity, optical path length (b = Δx) and the concentration of ethane. For methane-air and syngas-air mixtures, absorptance is calculated as the product of absorption coefficient, optical path length (b = Δx) and pressure. For carbon particles, absorptance is computed as the product of absorption coefficient and optical path length (b = Δx). In the 'upstream'subroutine, the individual absorptances of the two phases are added to obtain the absorptance of the dusty gas. The mixture specific heat $c_{p,mix}$ is calculated from the individual specific heats of the reactants [22].

The program CJwave is used with the subroutines of CHEMKIN and LSODE to calculate the downstream region. The subroutine 'upstream' is then used to calculate the flow properties in the upstream region. For baseline, the volume fraction of the solid particles in the fuel-air mixture is set to zero, which gives the flow characteristics of the fuel-air mixtures without solid particles. By varying the volume fraction, the calculations are repeated for dusty gas. Fig. 4 shows the flowchart for the computations. Initial conditions at the wave front (x = 0) are provided to CJwave. CJwave computes T_f, partial pressures of CO_2 and H_2O, and L, which are needed for the upstream calculations. The aforementioned parameters are the values attained when the solution in the downstream region converges. It sends these along with the initial conditions' information to 'upstream', which computes thermodynamic and flow properties of the upstream region. Here, the effect of the upstream properties on the shock wave and the downstream

calculations in determining the amount of heat release is not considered. This is due to the fact that increments in static temperature of about 5K were attained in the upstream region in all cases (refer results and discussion), which was considered to be trivial and not have any significant effect at the downstream end.

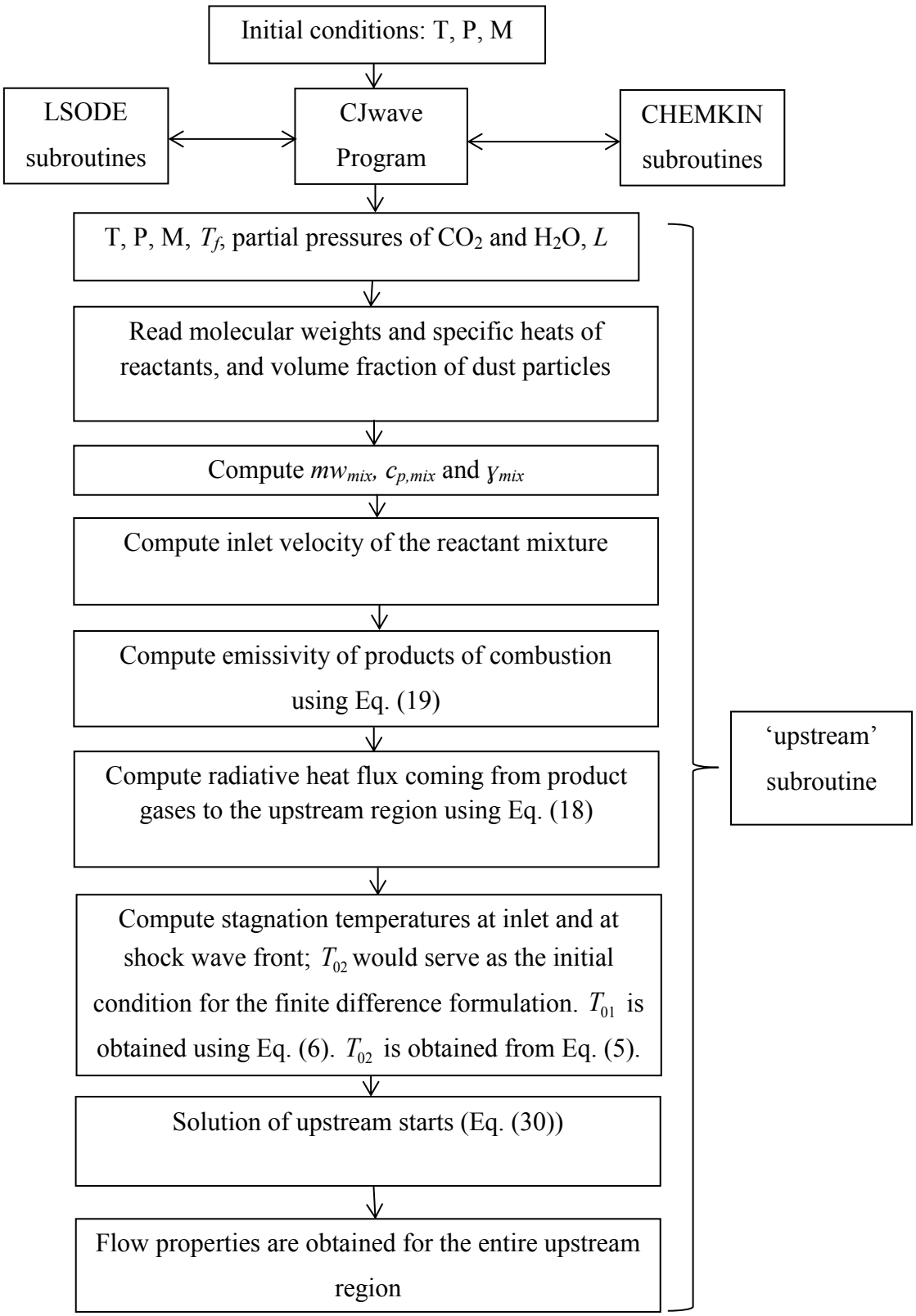

Fig. 4 Flowchart of main program and subroutines.

5. RESULTS AND DISCUSSION

CJwave along with the other subroutines was run for three fuel-air mixtures – ethane-air, methane-air and syngas-air, each at stoichiometric composition. The conditions at the upstream inlet for all the fuel-air mixtures were: T=300K, P=0.1 atm and M=7.4. These conditions are the same as those of Raghunandan [20]. The Mach number was selected so that it leads to attainment of equilibrium composition of species and flow properties in the downstream region. Volume fractions of carbon particles in the fuel-air mixtures used were: 0, 10^{-7}, 10^{-6} and 5×10^{-6}, constituting four sets of runs for each fuel-air mixture. The density and specific heat capacity of carbon particles used are 2,267 kg/m^3 and 710 J/kg-K, respectively. The molecular weight and specific heat capacity (at constant pressure) of the fuel-air mixture were calculated using the material properties of the individual reactants [22, 34] given in Table 1. A wavelength of 3 μm was considered to

Table 1 Material properties of reactants

Reactant	Molecular weight (kg/mol)	Specific heat capacity (J/kg-K)
Methane (CH_4)	0.016	2,220
Ethane (C_2H_6)	0.03	1,766
Nitrogen (N_2)	0.028	1,040
Oxygen (O_2)	0.032	919
Hydrogen (H_2)	0.002	14,320
Carbon monoxide (CO)	0.028	1,020
Carbon dioxide (CO_2)	0.044	844

determine the absorption coefficient of the carbon particles. The complex index of refraction used was m = 2.2-1.12i [28]. A step size Δx = 0.005 cm was used.

For each fuel-air mixture, plots that show variations of flow properties in downstream and upstream regions were made. For the downstream region, the flow variables T, ρ, P and M normalized against the inlet conditions were plotted vs. convective time, which is defined as the time a fluid particle takes to travel from the wave front (x = 0) to a given 'x' location [2]. Species mass fractions in the downstream region were also plotted against convective time. In the downstream region, as the carbon particles do not contribute significantly to the combustion process at the low volume fractions used in this work, the sets of flow properties and species mass fractions presented for each fuel-air mixture are for all the four values of the volume fractions. In the upstream region, variations of radiative heat flux and static temperature are shown vs. upstream distance from the wave front (x = 0). Variation of volume fraction of carbon particles affects heat absorption process in the upstream region, as would be observed in the graphical results.

A. Ethane-air mixture

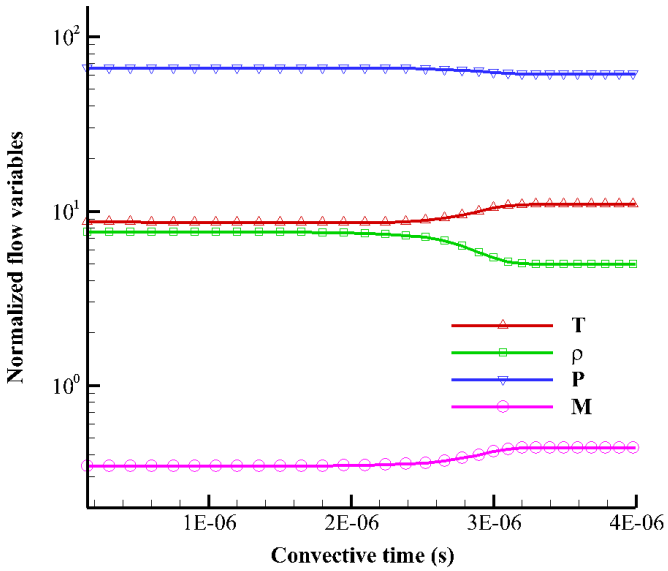

Fig. 5 Variation of flow properties in the downstream region for ethane-air mixture.

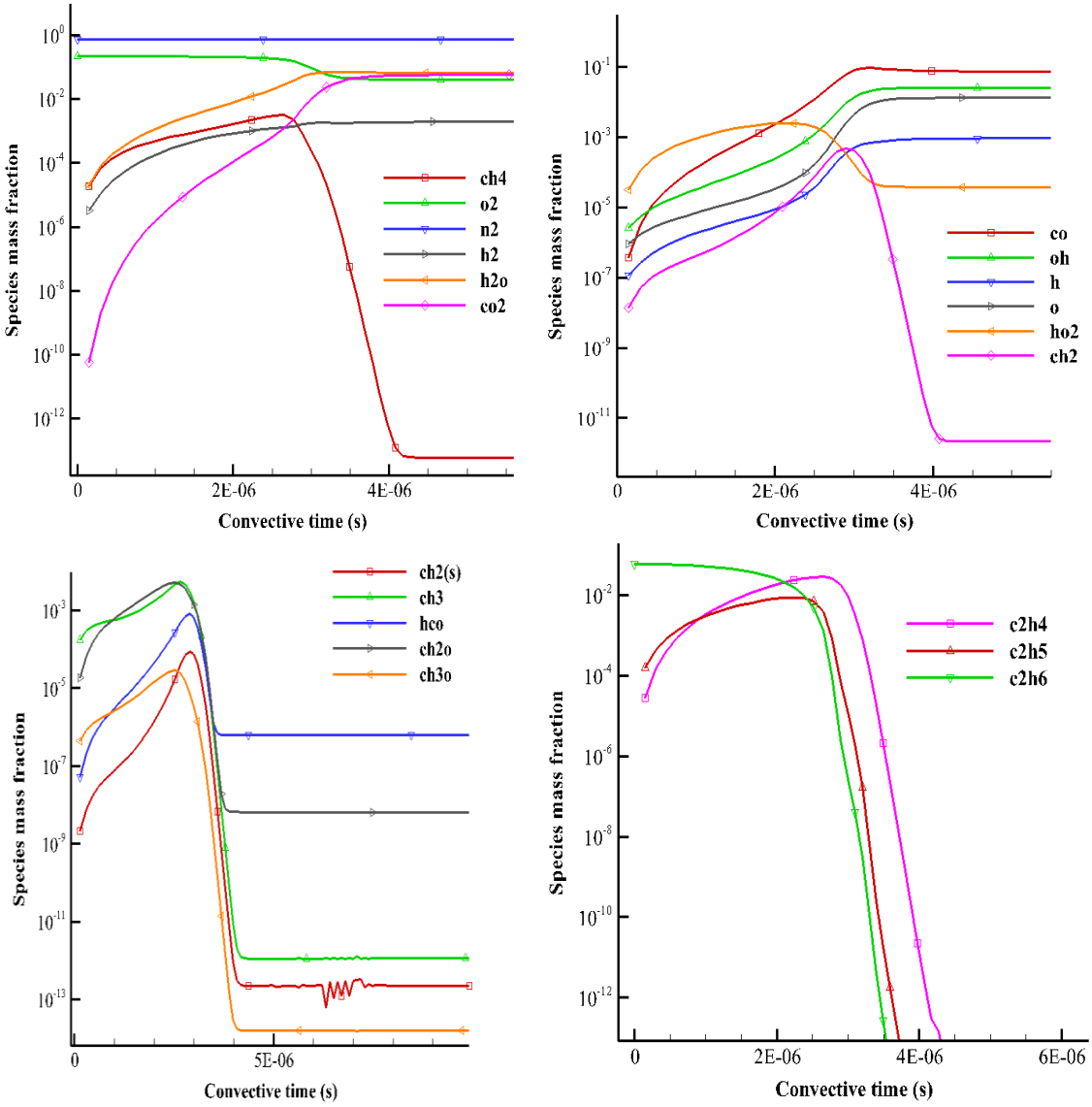

Fig. 6 Variation of mass fraction of species in the downstream region for ethane-air mixture.

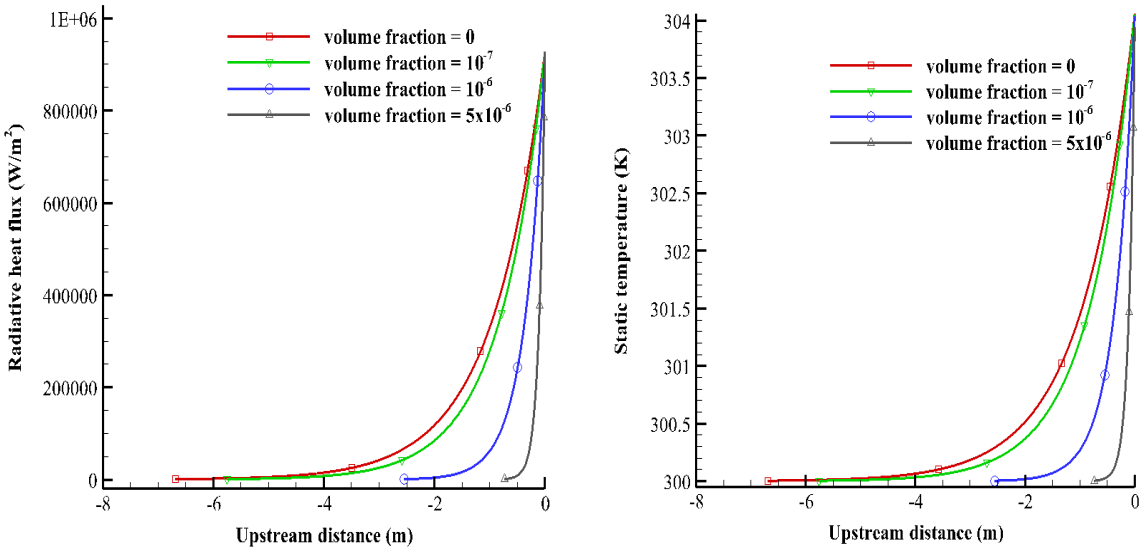

Fig. 7 Variation of radiative heat flux and static temperature in the upstream region for ethane-air mixture.

B. Methane-air mixture

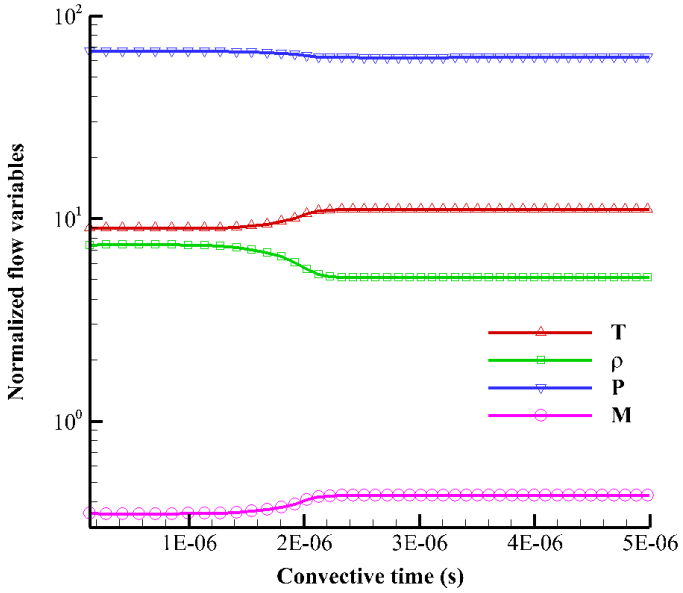

Fig. 8 Variation of flow properties in the downstream region for methane-air mixture.

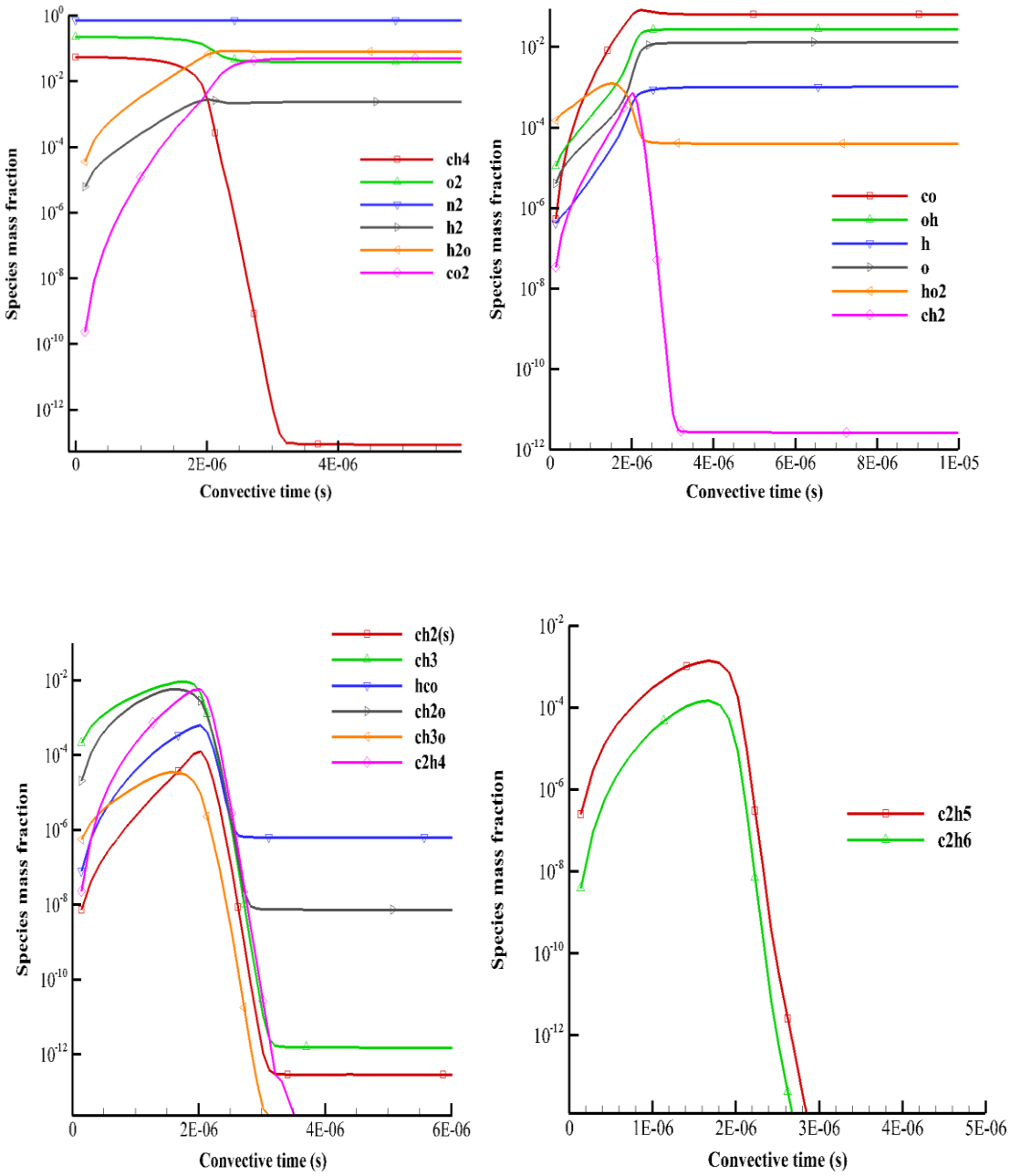

Fig. 9 Variation of mass fraction of species in the downstream region for methane-air mixture.

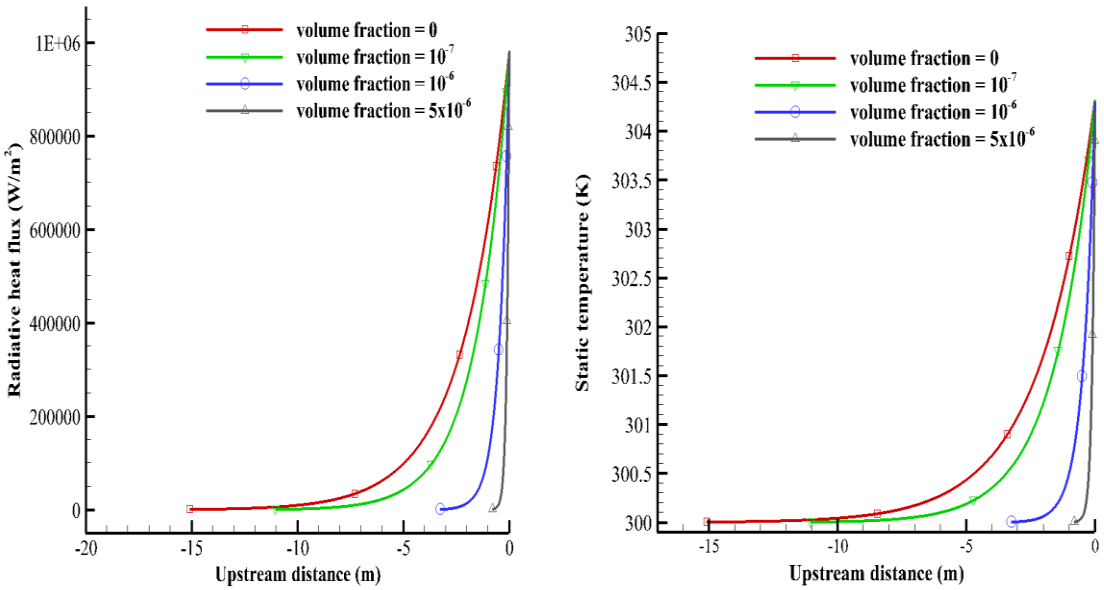

Fig. 10 Variation of radiative heat flux and static temperature in the upstream region for methane-air mixture.

C. Syngas-air mixture

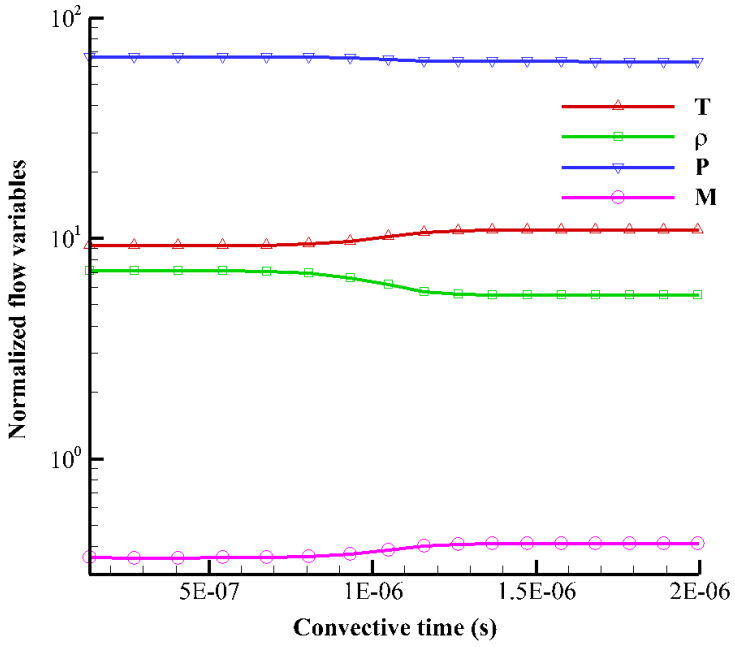

Fig. 11 Variation of flow properties in the downstream region for syngas-air mixture.

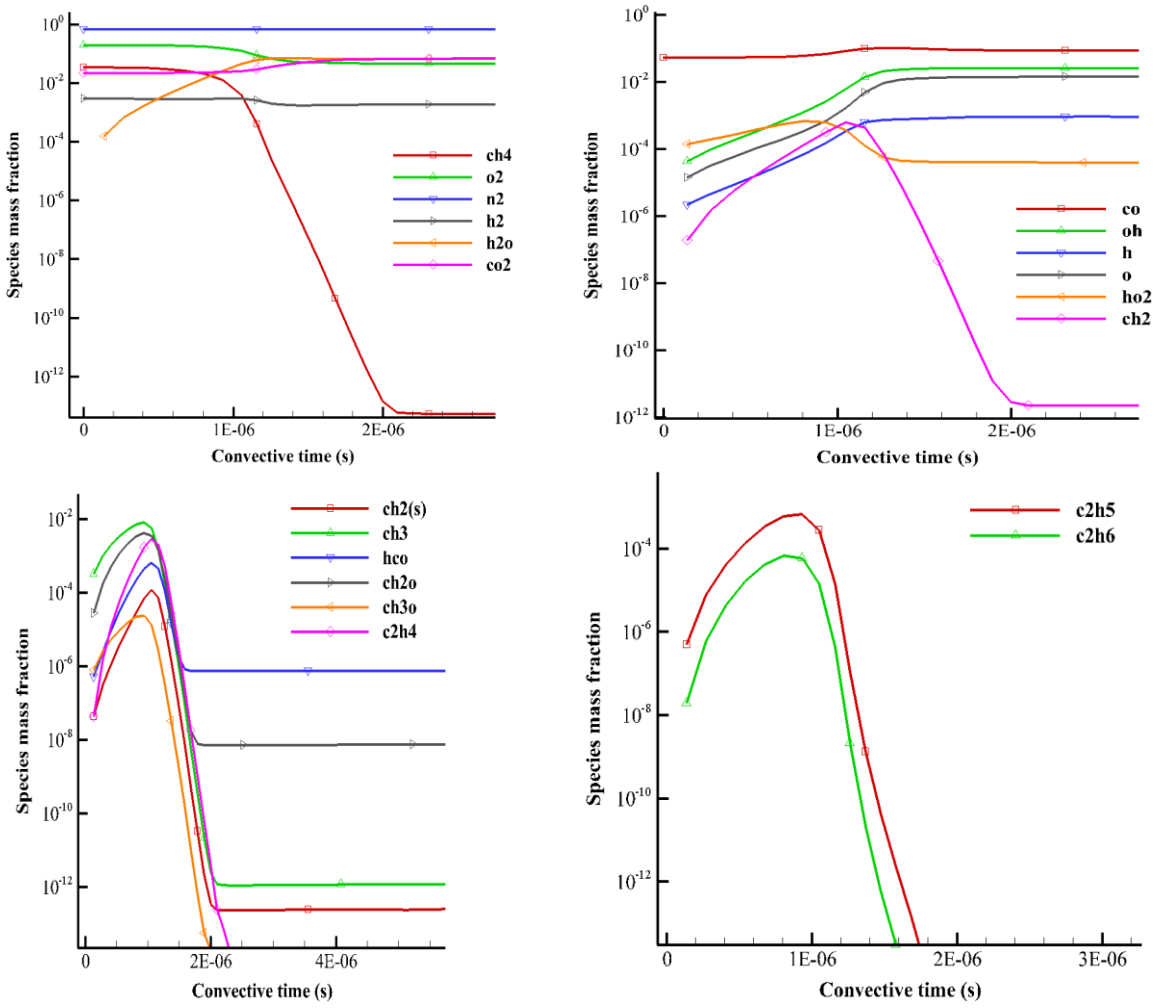

Fig. 12 Variation of mass fraction of species in the downstream region for syngas-air mixture.

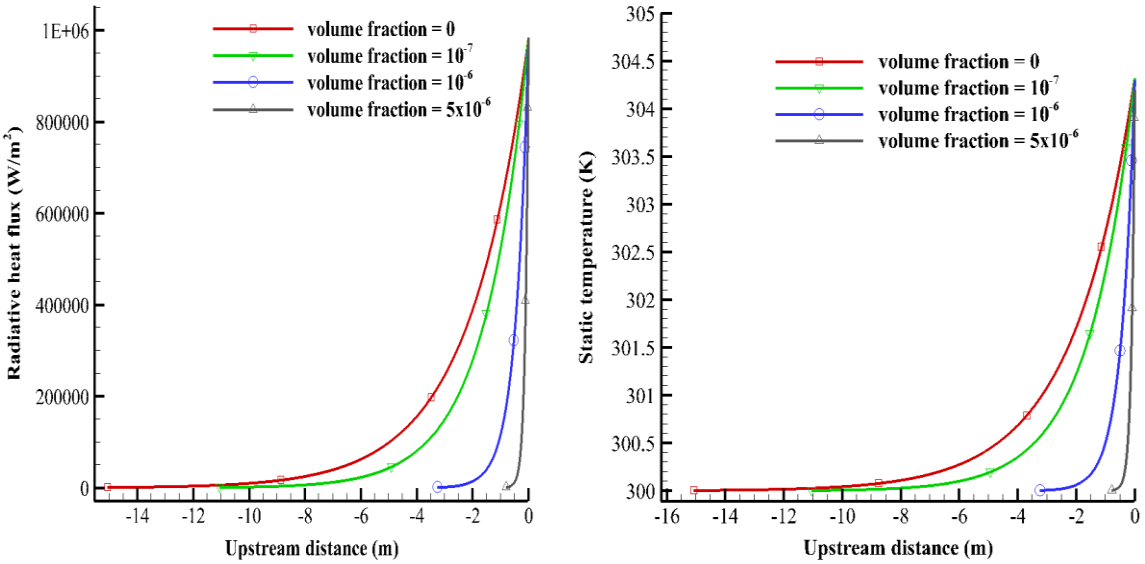

Fig. 13 Variation of radiative heat flux and static temperature in the upstream region for syngas-air mixture.

Figures 5, 8 and 11 show normalized flow variables vs. convective time for ethane-air, methane-air and syngas-air mixtures, respectively. The temperature and Mach number are gradually increasing whereas the density and pressure are gradually decreasing. In Figs. 5, 8 and 11, the flow variables start to level off around 4 μs, 3 μs and 1.5 μs, respectively. For ethane-air mixture, the trend in flow properties is similar to that obtained by Raghunandan [20]. In Fig. 8, the trend is similar to that obtained by Isaac and Scott [2], where methane-air mixture is at an inlet pressure of 1 atm. The variations in temperature and pressure in the downstream region are also in agreement with that of frictionless flow in a constant-area duct, in which stagnation temperature change occurs [22]. Combustion is a process that involves change of stagnation temperature. In the aforementioned plots, the flow is initially subsonic and the Mach number is approaching unity. When the flow becomes sonic, it is termed thermally choked, a condition in which stagnation conditions would not change until the inlet conditions change.

Figures 6, 9 and 12 show species mass fractions vs. convective time for ethane-air, methane-air and syngas-air mixtures respectively. Here the profiles of unburned reactants (fuel, O_2 and N_2) and major combustion products (CO_2 and H_2O) are primarily discussed. Mass fraction of N_2, which is an inert species, remains constant for all fuel-air mixtures. In Fig. 6, mass fraction of C_2H_6 keeps decreasing and before 4 μs, it drops below 10^{-12}. For O_2, its mass fraction keeps decreasing and around 4 μs it starts to level off. CO_2 and H_2O profiles reach their peaks at 4 μs and 3 μs, respectively, and thereafter level off. By 5 μs, the remaining species mass fraction profiles reach either steady state or relatively very small levels. In the work by Raghunandan [20], around 3 μs, C_2H_6 and O_2 get consumed almost entirely and mass fractions of CO_2 and H_2O level off. Figure 9 shows that CH_4 and O_2 keep getting consumed and around 4 μs and 3 μs, respectively, they start to stabilize. CO_2 and H_2O mass fractions reach their peak values at nearly 3 μs and 2 μs respectively and thereafter level off. Apart from a few species, the remaining species reach a steady state at 4 μs. In Fig. 12, mass fraction of H_2 keeps decreasing and it levels off at 1.5 μs. CO and C_2H_6 profiles reach a peak, then fall and become even at nearly 2 μs. O_2 and CH_4 show a decreasing trend and start to level off at nearly 1.5 μs and 2 μs. CO_2 and H_2O profiles reach their maximum value and level off at nearly 2 μs. Nearly all of the remaining species reach steady state within 2 μs.

In Figs. 7, 10 and 13, the distance is measured with reference to the wave front. The negative values on the horizontal axis indicate distance measured in the negative x-direction. The radiative heat flux at the wave front for all the fuel-air mixtures is greater than 9×10^5 W/m^2. In all the cases, radiative heat flux and static temperature are gradually decreasing with increasing distance in the upstream direction. It is an indication

that heat radiated from the downstream region is gradually being absorbed in the upstream region. The distance from the wave front to the upstream location, where 99.99 percent of the amount of heat radiated from the combustion products was absorbed, is defined as the absorbing distance. Table 2 shows the absorbing distances for the fuel-air mixtures with varying proportions of carbon particles. For ethane-air mixture, an absorbing distance close to 6 m was obtained by Raghunandan [20]. The differences between Raghunandan [20] and the present work are probably due to the use of stagnation temperature in the present formulation vs. static temperature by Raghunandan [20]. The present method appears to be an improvement over the method of Raghunandan [20], since the static temperature profiles have their slopes tending to zero toward termination of the computations, as expected, since less radiated heat is available for absorption as the upstream distance increases. Also, as expected, as the volume fraction of the carbon particles in the fuel-air mixture increases, the absorbing distance decreases. The numerical model for the upstream region does not consider the impact of the change in the absorbing distance on the detonation wave. The trends in Figs. 10 and 13 show that, for methane-air and syngas-air, a reduction in absorbing distance by ~10m is possible by having a carbon particle volume fraction of $5x10^{-6}$.

Table 2 Absorbing distances for fuel-air mixtures

Fuel-air mixture	Volume fraction of carbon particles	Absorbing distance (m)
C_2H_6-air	0	6.685
	10^{-7}	5.753
	10^{-6}	2.551
	5×10^{-6}	0.734
CH_4-air	0	15.066
	10^{-7}	11.037
	10^{-6}	3.239
	5×10^{-6}	0.782
Syngas-air	0	15.066
	10^{-7}	11.037
	10^{-6}	3.239
	5×10^{-6}	0.782

D. Downstream path length studies

In Eq. (19), the emissivity is calculated by using the path length in the downstream region. Subsequently, the radiative heat flux at the shock wave front is obtained. A path length variation study was done for each of the fuel-air mixtures without the carbon particles to see how changes in path length affect the heat flux into the upstream region. Computations were done for two sets of path lengths (1.1m and 10m) and the results are shown in Fig. 14. 10 m was chosen to determine how such a big change can affect the heat transfer process. The corresponding absorbing distances, radiative heat flux and static temperature at the shock wave front are shown in Table 3.

1. Ethane-air mixture

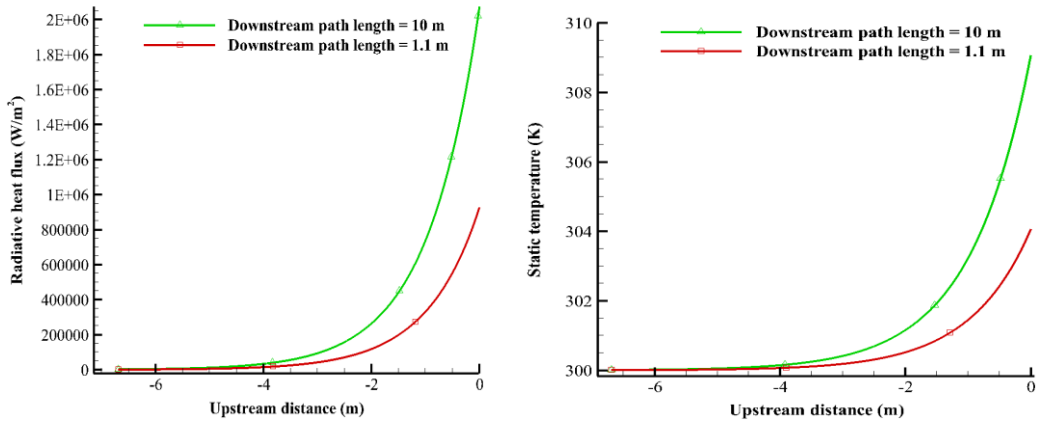

2. Methane-air mixture

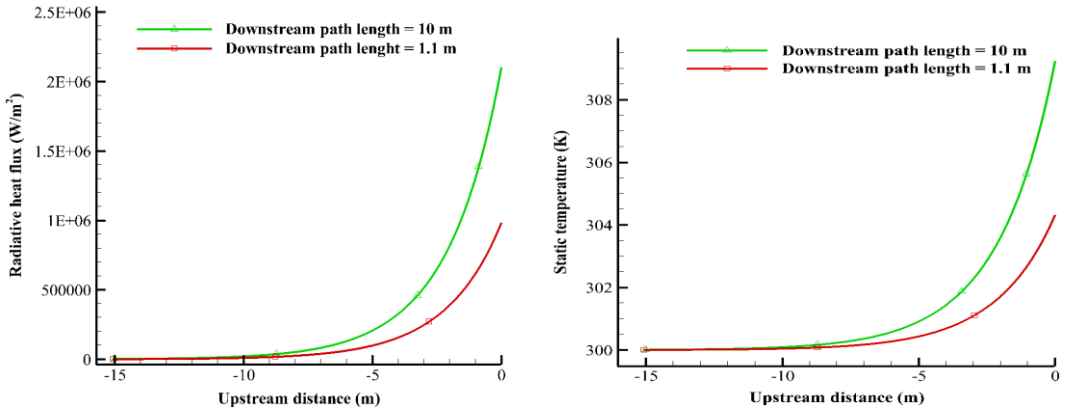

3. Syngas-air mixture

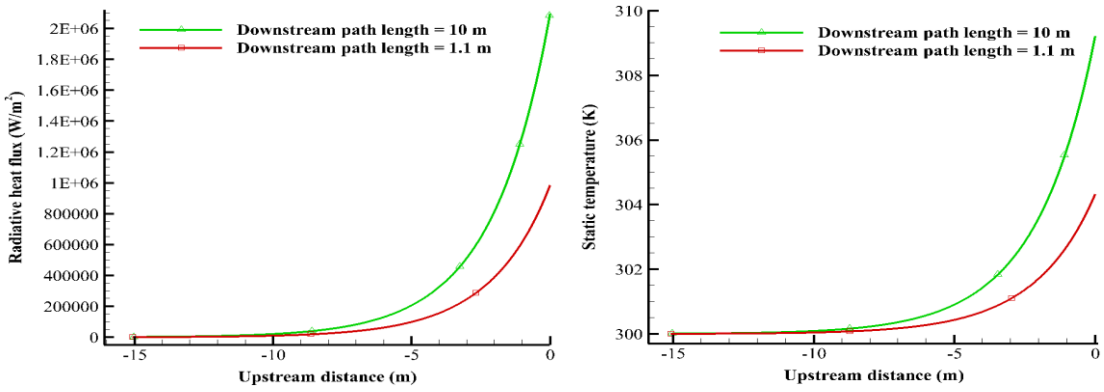

Fig 14. Variations of radiative heat flux and static temperature in the upstream region due to variations in path length in the downstream region.

Table 3 Absorbing distances and properties at shock wave front for fuel-air mixtures

Fuel-air mixture	Path length (m)	Absorbing distance (m)	Radiative heat flux at shock wave front (W/m^2)	Static temperature at shock wave front (K)
C_2H_6-air	10	6.686	2,074,594	309.07
	1.1	6.685	928,619	304.06
CH_4-air	10	15.015	2,100,556	309.25
	1.1	15.066	982,579	304.33
Syngas-air	10	15.016	2,096,614	309.21
	1.1	15.066	984,316	304.32

For all the fuel-air mixtures, it was observed that the absorbing distance is almost the same for both path lengths. However, compared to path length of 1.1 m, radiative heat flux nearly doubled and static temperature increased by about 5 K in the case of path length of 10 m. Absorbing distance did not change much because absorptance remains almost same for both path lengths. Due to the nature of the dependence of absorptivity models on static temperature, the absorptance did not change much between the two path lengths. Interpreted differently, regardless of the magnitude of the heat flux at the wave front, the same fraction of energy is absorbed over a given length of the upstream region, and the length required to absorb most of the heat radiated from the downstream region remains almost the same. In Tables 2 and 3, identical results were obtained in the case of methane-air and syngas-air. This can be attributed to the fact that for both fuel-air mixtures the same absorptivity model was used, which consists of absorption coefficient of the same hydrocarbon fuel, i.e. methane.

6. CONCLUSION

The present study primarily investigated absorption of the heat generated by the products of combustion produced in detonations, by the unburned gas-solid mixtures. In addition, the physics of the combustion process were also studied in detail. The fuels used comprised ethane, methane and syngas, in a stoichiometric composition with air, seeded with carbon particles to form dusty gas mixtures. A set of codes, some developed in-house and others available from other sources, were run together as a package to provide insight into the radiative heating of gases upstream of a detonation wave. Spatial variation of heat flux, produced by combustion products, into unburned fuel in the upstream region, and the corresponding static temperature rise showed the effect of varying the volume fraction of carbon particles in the gaseous hydrocarbon fuels. This dusty gas mixture is observed to be a stronger absorber of the incoming heat indicated by the shorter absorbing length at higher particle volume fractions. Variations of temperature, density, pressure, Mach number and species mass fractions depict the processes taking place immediately downstream of the wave front consisting of an induction region, ignition point, heat release zone and an equilibrium zone. The downstream region consists of a subsonic region where heat release due to combustion causes the Mach number to increase and eventually become unity indicating thermal choking, characteristic of the Rayleigh process. A study of path length of the burned product gas revealed how it plays a significant role in the amount of heat generated during combustion.

Rise in static temperature at the shock wave front of the upstream region of up to ~10K was observed in certain cases. Adding small carbon particles to the gas mixture to

increase the absorptivity of the mixture showed significant shortening of the absorption length. This has technological importance since particles can be deliberately added to control absorption length such as in pulse detonation engines, or how the presence of dust particles in gas mixtures affect their explosive properties such as encountered in mines.

APPENDIX

Table 4 shows the value of the coefficients required to use Eq. (22).

Table 4 Value of the coefficients used to determine methane's absorption coefficient

Coefficients	Values
a_0	-1.8267×10^{-5}
a_1	3.9617×10^{-7}
a_2	-7.7619×10^{-10}
a_3	5.7857×10^{-13}
a_4	-1.5283×10^{-16}
R^2	9.9196×10^{-1}

Table 5 shows the composition of the syngas in terms of volume percentage.

Table 5 Composition of syngas

Components	Volume percentage
Hydrogen (H_2)	18.0
Carbon monoxide (CO)	24.0
Carbon dioxide (CO_2)	6.0
Oxygen (O_2)	0.4
Methane (CH_4)	27.0
Nitrogen (N_2)	24.6
Ethane (C_2H_6)	0.0

ACKNOWLEDGMENTS

Graduate teaching assistantship provided by the Missouri S&T is gratefully acknowledged by the first author. The FORTRAN code 'CJwave' was originally written by J. Zhao, and later versions coded by B. Li and B. Crabtree.

REFERENCES

[1] Kailasanath, K., "Review of Propulsion Applications of Detonation Waves," AIAA Journal, Vol. 38, No. 9, 2000, pp. 1698-1708.

doi: 10.2514/2.1156

[2] Isaac, K. M., and Scott, T., "Ignition delay and detonation wave structure using detailed chemical kinetics models," 2nd U. S. Sections Joint Meeting of the Combustion Institute, Oakland, CA, March 25-28, 2001.

[3] Griner, J., and Isaac, K. M., "Induction Time and Detonation Wave Structure of Acetylene, Ethylene and JP-10," Proceedings of the 2002 Technical Meeting of the Central States Section of the Combustion Institute, 2002.

[4] Ivanov, M. F., Kiverin, A. D., and Liberman, M. A., "Ignition of Deflagration and Detonation Ahead of the Flame due to Radiative Preheating of Suspended Micro Particles," arXiv, Cornell University, Ithaca, NY, 2014 (unpublished).

[5] Karlin, V., "Radiation Preheating can Trigger Transition from Deflagration to Detonation," Flow Turbulence Combust, Vol. 87, No. 2-3, 2011, pp. 511–523.

doi: 10.1007/s10494-010-9317-9

[6] Oran, E. S., "The structure of propagating detonations: Lessons from numerical simulations," Laboratory for Computational Physics and Fluid Dynamics, Naval Research Laboratory, Washington, DC, 1999.

[7] Nikolaev, Y. A., Vasil'ev, A. A., and Ul'yanitskii, B. Y., "Gas Detonation and its Application in Engineering and Technologies (Review)," Combustion, Explosion, and Shock Waves, Vol. 39, No. 4, 2003, pp. 382-410.

doi: 10.1023/A:1024726619703

[8] Shepherd, J. E., "Detonation in gases," Proceedings of the Combustion Institute, Vol. 32, No. 1, 2009, pp. 83–98.

doi: 10.1016/j.proci.2008.08.006

[9] Bdzil, J. B., and Davis, W. C., "Time-Dependent Detonations," Los Alamos Scientific Laboratory of the University of California, Los Alamos, New Mexico, 1975.

[10] Veyssiere, B., "Detonations in Gas-Particle Mixtures," Journal of Propulsion and Power, Vol. 22, No. 6, 2006, pp. 1269-1288.

doi: 10.2514/1.18378

[11] Roy, G. D., Frolov, S. M., Borisov, A. A., and Netzer, D. W., "Pulse detonation propulsion: challenges, current status,and future perspective," Progress in Energy and Combustion Science, Vol. 30, No. 6, 2004, pp. 545–672.

doi: 10.1016/j.pecs.2004.05.001

[12] Heaslet, M. A., and Baldwin, B. S., "Predictions of the Structure of RadiationResisted Shock Waves," Physics of Fluids, Vol. 6, No. 6, 1963, pp. 781-791.

doi: 10.1063/1.1706814

[13] Zel'dovich, Ia. B., "Shock Waves of Large Amplitude in Air," Soviet Physics JETP, Vol. 5, No. 5, 1957, pp. 919-927.

[14] Pearson, W. E., "On the direct solution of the governing equation for radiation-resisted shock waves," NASA TN D-2128, Washington, 1964.

[15] Clarke, J. F., "Radiation-Resisted Shock Waves," Physics of Fluids, Vol. 5, No. 11, 1962, pp. 1347-1361.

doi: 10.1063/1.1706530

[16] Olfe, D. B., and Cavalleri, R. J., "Shock Structure with Non-Gray Radiative Transfer," Proceedings of the 1967 Heat Transfer and Fluid Mechanics Institute, 1967, pp. 88-108.

[17] Emanuel, G., "Structure of Radiation-Resisted Shock Waves with Vibrational Nonequilibrium," Physics of Fluids, Vol. 8, No. 4, 1965, pp. 626-635.

doi: 10.1063/1.1761275

[18] Drake, R. P., "Theory of radiative shocks in optically thick media," Physics of Plasmas, Vol. 14, No. 4, 2007.

doi: 10.1063/1.2716639

[19] Buckley Jr., F. T., "Radiation-resisted shock waves in gas-particle flows," AIAA Journal, Vol. 9, No. 8, 1971, pp. 1603-1607.

doi: 10.2514/3.6394

[20] Raghunandan, P., "Gray gas analysis of radiative preheating effects on shock induced combustion," M.S. Thesis, Department of Mechanical and Aerospace Engineering, Missouri University of Science and Technology, Rolla, MO, 2012.

[21] Raghunandan, P., and Isaac, K. M., "Numerical Study of Upstream Radiative Heating in 1-D Detonations," 51st AIAA Aerospace Sciences Meeting including the New Horizons Forum and Aerospace Exposition, AIAA, Grapevine (Dallas/Ft. Worth Region), TX, 2013.

doi: 10.2514/6.2013-738

[22] Hill, P. G., and Peterson, C. R., Mechanics and Thermodynamics of Propulsion, 2nd ed., Addison-Wesley Publishing Company, 1992, Chaps. 2, 3.

[23] Brennen, C. E., Fundamentals of Multiphase Flows, Cambridge University Press, 2005, Chap. 11.

[24] Coppalle, A., and Vervisch, P., "The Total Emissivities of High-Temperature Flames," Combustion and Flame, Vol. 49, Nos. 1-3, 1983, pp. 101-108.

doi: 10.1016/0010-2180(83)90154-2

[25] Olson, D. B., Mallard, W. G., and Gardiner, J. W. C., "High Temperature Absorption of the 3.39 μm He-Ne Laser Line by Small Hydrocarbons," Applied Spectroscopy, Vol. 32, No. 5, 1978, pp. 489-493.

[26] Wakatsuki, K., "High Temperature Radiation Absorption of Fuel Molecules And An Evaluation of Its Influence on Pool Fire Modeling," Ph.D. Dissertation, Department of Mechanical Engineering, University of Maryland, College Park, MD, 2005.

[27] Lanzo, C. D., and Ragsdale, R. G., "Heat transfer to a seeded flowing gas from an arc enclosed by a quartz tube," NASA Lewis Research Center, Cleveland, Ohio.

[28] Modest, M. F., Radiative Heat Transfer, 3rd ed., Elsevier Science and Technology Books, 2013,Chap. 12.

[29] Viskanta, R., and Menguc, M. P., "Radiation heat transfer in combustion systems," Progress in energy and combustion science, Vol. 13, 1987, pp. 97-160.

doi: 10.1016/0360-1285(87)90008-6

[30] Zhao, J., "CJWave-Performs detailed analysis of flow across a Chapman-Jouguet wave and combustion downstream," Department of Mechanical and Aerospace Engineering, Missouri University of Science and Technology, Rolla, MO, 1991.

[31] Hindmarsh, A. C., "Livermore Solver For Ordinary Differential Equations," Mathematics and Statistics Section, L-300, Lawrence Livermore Laboratory, Livermore, CA, 1980.

[32] Kee, R. J., Miller, J., and Jefferson, T. H., "CHEMKIN: A General-Purpose, Problem-Independent, Transportable, Fortran Chemical Kinetics Code Package," Sandia National Laboratories Report SAND80-8003, 1980.

[33] Frenklach, M., and Kazakov, A., http://www.me.berkeley.edu/drm/.

[34] Turns, S. R., An Introduction to Combustion, 2nd ed., McGraw-Hill, 2000, Chap. 2.

APPENDIX A.

CASE STUDY OF ACETYLENE OXYGEN MIXTURES

NOMENCLATURE

Symbol		Description
L	=	path length of gas in the downstream region, m
M	=	Mach number
P	=	pressure, atm
P_{tot}	=	total pressure of combustion products, atm
T	=	temperature, K

Subscript

f	=	flame

1. INTRODUCTION

For detonation combustion, specifically in a PDE, acetylene is considered as a readily detonable fuel [2-4]. Griner and Isaac [5] conducted one dimensional numerical simulation of detonation with detailed chemical kinetics and obtained ignition delay and wave structure of acetylene. In the present work, a case study was done by using acetylene-oxygen as the fuel oxidizer mixture. Proportions of carbon particles, that were used to study dusty gas mixtures of ethane, methane and syngas, were used for acetylene-oxygen too. Simulations of the three fuel-air mixtures, mentioned in the included manuscript, used DRM 19 mechanism which is a subset of the GRI-MECH 1.2 mechanism [6]. Variations in flow properties and species' composition in the downstream region were obtained through CJwave [7]. DRM 19 mechanism has the species methane,

ethane and the individual components of syngas (refer the manuscript for details), so it was used for their fuel-air mixtures. It does not have the species acetylene. So, downstream calculations could not be performed for acetylene. It could have been done using a different reaction mechanism, with the number of species involved within the limit that can be handled by CJwave. Unfortunately, due to lack of time it could not be done. Similar to 'upstream' a separate and independent code, which can be run without being integrated with CJwave and other subroutines, was made. It provides the flow properties' variation in the upstream region. The only differences it has when compared to 'upstream' is that the parameters flame temperature, downstream path length and total pressure of combustion products have to be provided by the user; other than that it follows the same algorithm as 'upstream'. In 'upstream' the three aforementioned parameters are computed and provided to it by CJwave. To avoid any kind of confusion, the results from the acetylene-oxygen case study were not included in the manuscript.

2. FLAME TEMPERATURE OF ACETYLENE OXYGEN MIXTURE

Flame temperature, required as an input in the code for acetylene-oxygen mixture, was obtained by using an online adiabatic flame temperature calculator [8]. A stoichiometric mixture of acetylene and oxygen at 0.1 atm and 300K was considered. It uses GRI-MECH 3.0, a chemical kinetics scheme, to determine the composition of the product mixture by including both major and minor species. It resulted in a flame temperature of 3005.34 K.

3. RESULTS AND DISCUSSION

The code was run using the initial conditions of the mixture, i.e. T = 300 K, P = 0.1 atm and M = 7.4, and L = 1.1 m, P_{tot} = 6.24 atm and T_f = 3005.34 K. Absorptivity of acetylene used was 1.6 X 10 ^{3} cm^2/mol. The initial conditions and downstream path length were kept same as those for the fuel-air mixtures mentioned in the manuscript. Total pressure of combustion products of methane-air mixture was used here. Radiative heat flux and static temperature distributions obtained for the upstream region are shown in Figure 3.1.

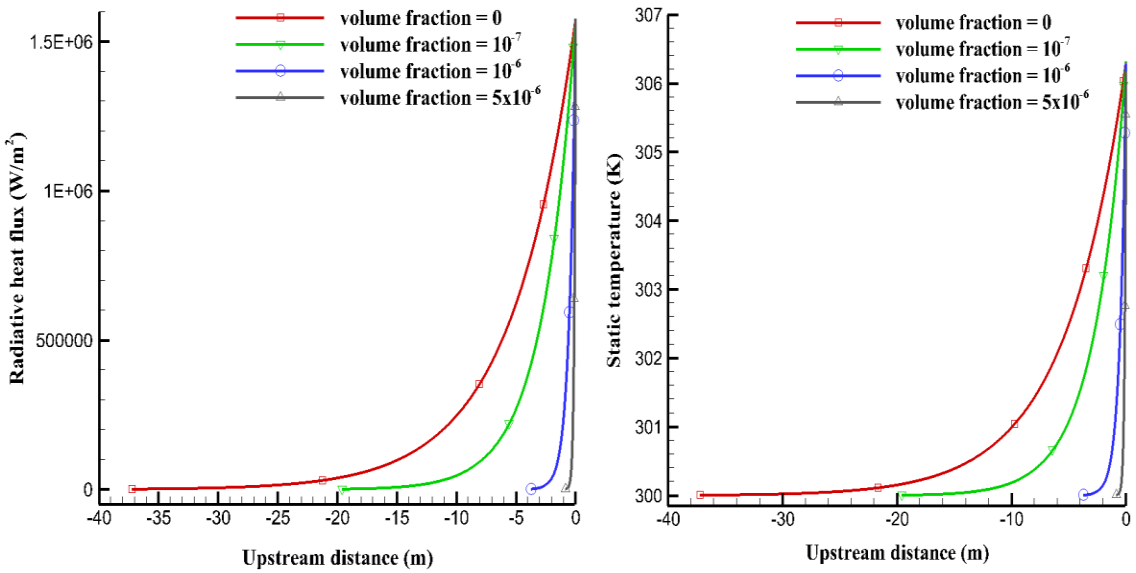

Figure 3.1. Variations of radiative heat flux and static temperature in the upstream region for acetylene-oxygen mixture.

In Figure 3.1, volume fraction refers to the proportion of carbon particles in the acetylene-oxygen mixture. '0' indicates the shock wave front. Radiative heat flux at the shock wave front is 1.57684 x 10^6 W/m^2. Case study done with a volume fraction of zero was the base line case. Static temperature at the shock wave front for the base line case was 306.317 K. The distance from the shock wave front to the upstream location, where 99.99 percent of the amount of heat radiated from the combustion products is absorbed, is considered as the absorbing distance. Table 3.1 shows the absorbing distances for the acetylene-oxygen mixture with varying proportions of carbon particles.

Table 3.1. Absorbing distances for acetylene-oxygen mixtures

Volume fraction	Absorbing distance (m)
0	37.1945
10^{-7}	19.56195
10^{-6}	3.7142
$5x10^{-6}$	0.8072

It was observed from Table 3.1 that upon increasing volume fraction of carbon particles, absorbing distance was decreasing.

4. DOWNSTREAM PATH LENGTH STUDIES

In the manuscript study of downstream path length variation for the three fuel-air mixtures were done and presented. For the same reasons (refer manuscript), a downstream path length variation study of acetylene-oxygen mixture was also done for

two sets of path lengths, as shown in Figure 4.1. In Figure 4.1 '0' on the horizontal axis indicates the shock wave front.

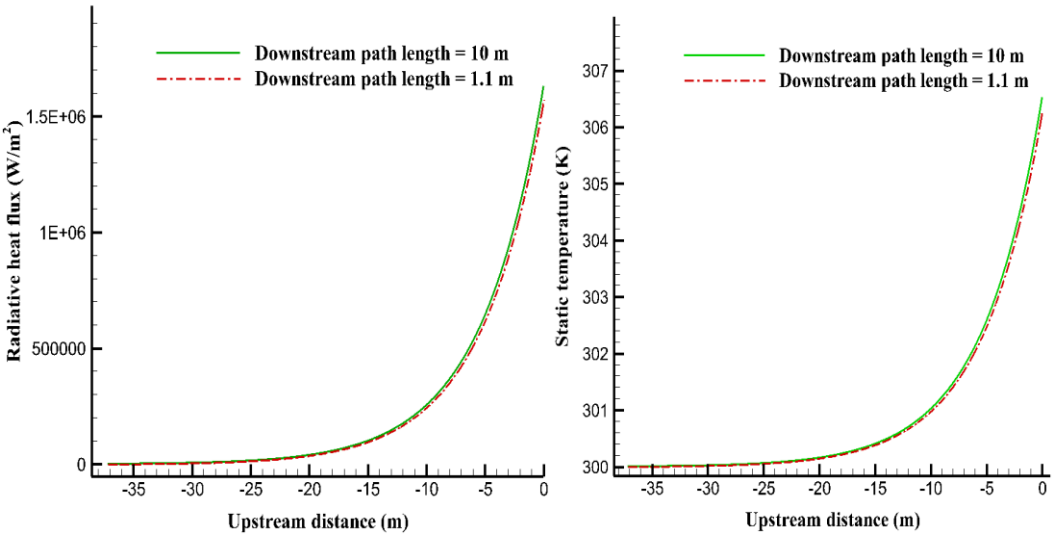

Figure 4.1. Variations of radiative heat flux and static temperature in the upstream region due to variations in path length in the downstream region, for acetylene oxygen mixture.

The corresponding absorbing distances, radiative heat flux and static temperature at the shock wave front are shown in Table 4.1, and they do not differ much for the two path lengths. In Figure 4.1 the two curves are almost coincident. When compared to the fuel-air mixtures (refer manuscript), the trend for absorbing distance is similar, whereas, for radiative heat flux and static temperature at wave front there is appreciable difference. Radiative heat flux is calculated by using equation 18 (in manuscript). It depends on flame temperature and emissivity of combustion products. Flame temperatures of all fuel-oxidizer mixtures were found to be around 3000 K. The emissivity model used here [9]

has an exponential dependence on the pressure –path length product, where the pressure term is the sum of partial pressures of water vapor and CO_2. Fuel-air mixtures, mentioned in the manuscript, comprised of several other species in the burned products other than water vapor and CO_2. CJwave computed the products' composition. In case of acetylene-oxygen mixture, as CJwave was not involved, so, the products were considered to be consisting of only CO_2 and water vapor. Sum of partial pressure of CO_2 and water vapor was much higher than that of any of the fuel-air mixtures. So, at high pressure values, change in path length did not affect emissivity and therefore radiative heat flux remained almost same. Consequently, static temperature at shock wave front was not affected much.

Table 4.1. Absorbing distances and properties at shock wave front for acetylene oxygen mixture

Path length (m)	Absorbing distance (m)	Radiative heat flux at shockwave front (W/m^2)	Static temperature at the shockwave front (K)
10	37.19445	1,631,397.99	306.53
1.1	37.1945	1,576,836.92	306.32

APPENDIX B.

FORTRAN SUBROUTINE TO INVESTIGATE UPSTREAM REGION

```
!-----------------------------------------------------------------------------------------------------------
! Abstract - Subroutine 'UPSTREAM' is used to compute spatial variation of flow properties
! in the upstream region of a one dimensional detonation of gas-particle mixture or dusty gas
!
!                          Shubhadeep Banik
!                          Missouri S&T 2014
!-----------------------------------------------------------------------------------------------------------
SUBROUTINE UPSTREAM(T1,P1,M1,TF,PTOT,L,Q,N,FINXS)
! Units are in parenthesis
!-----------------------------------------------------------------------------------------------------------
! Variables
! T1 = initial temperature of reactant mixture (K)
! P1 = initial pressure of reactant mixture (atm)
! M1 = initial Mach number of reactant mixture
! TF = flame temperature of gases in the downstream region (K)
! PTOT = total pressure of gases in the downstream region (atm)
! L = path length of gases in the downstream region (m)
! Q = radiative heat flux (W/m^2)
! N = index
! FINXS = mole fraction of species at the end of combustion
!-------------------------------------------------------------------
INTEGER I,N,G,J,NR,FUEL
DOUBLE PRECISION SIGMA,TF,EPSTOT,QR,T1,P1,M1,T01,GAMMA,RHO1,R,V1
DOUBLE PRECISION DELTAT0,T02,T2,M2,ABSORPTIVITY(2000000),P(2000000)
DOUBLE PRECISION P2,RU,D,B,A,Q(2000000),T(2000000),CONC(2000000)
DOUBLE PRECISION RHO(2000000),U(2000000),T0(2000000),KP(2000000)
DOUBLE PRECISION C(2000000),K,K2,K1,CS1,C2,MSQ1(2000000),MSQ2(2000000)
DOUBLE PRECISION M(2000000),ABSORPTANCE(2000000),P0(2000000),MWMIX
DOUBLE PRECISION TOL,ERROR,QT,QSUM,QABSD(2000000),C1,CC1,CC2,KK2,KK1
DOUBLE PRECISION PTOT,PPWAT,PPCDX,PL,L,KI(4),ALPHA(4),BETA(4),KK,AK
DOUBLE PRECISION BK,DK,MS1,MS2,PPRATIO,P01,MW(10),NM(10),CP(10),MF(10)
DOUBLE PRECISION TOTMOL,FINXS(22),VOLFRAC,ABSORPTANCEC(2000000)
DOUBLE PRECISION RHOE1,GAMMAE,CPE,CS1E,V1E,RE,CPMIX,ABSORPTANCED
```

```
OPEN (UNIT = 8,   FILE = 'X.DAT' ,          STATUS = 'REPLACE')
OPEN (UNIT = 9,   FILE = 'P.DAT' ,          STATUS = 'REPLACE')
OPEN (UNIT = 10, FILE = 'M.DAT' ,          STATUS = 'REPLACE')
OPEN (UNIT = 11, FILE = 'DU.DAT',          STATUS = 'REPLACE')
OPEN (UNIT = 15, FILE = 'input.dat' ,       STATUS = 'OLD',ACTION='READ')
OPEN (UNIT = 16, FILE = 'T.DAT' ,          STATUS = 'REPLACE')
OPEN (UNIT = 17, FILE = 'T0.DAT' ,         STATUS = 'REPLACE')
OPEN (UNIT = 18, FILE = 'P0.DAT' ,         STATUS = 'REPLACE')
OPEN (UNIT = 19, FILE = 'Q.DAT' ,          STATUS = 'REPLACE')
OPEN (UNIT = 20, FILE = 'ABSORPTANCE.DAT' , STATUS = 'REPLACE')

! Converting to SI units
P1=P1*101325.0D+00 ! (Pascal)
RU = 8.314 ! Gas constant(J/K-mol)

! Reading from file 'input.dat': no. of reactant, molecular weight, no. of moles of each
! Reactant, specific heat of each reactant, volume fraction of carbon particles, type of fuel
READ(15,*) NR
READ(15,*) (MW(J),J=1,NR)
READ(15,*) (NM(J),J=1,NR)
READ(15,*) (CP(J),J=1,NR)
READ(15,*) VOLFRAC
READ(15,*) FUEL

! Computing mole fraction of each reactant in the reactant mixture
TOTMOL = 0
  DO 8 J = 1,NR
    TOTMOL = TOTMOL +NM(J)
8  CONTINUE
  DO 9 J = 1,NR
    MF(J) = NM(J)/TOTMOL
9  CONTINUE

! Computing reactant mixture molecular weight
```

```
! Ref: Turns, S. R., An Introduction to Combustion, 2nd ed.,
! McGraw-Hill, 2000, Chap. 2.
MWMIX = 0
  DO 10 J = 1,NR
    MWMIX = MWMIX + (MF(J)*MW(J))
10 CONTINUE

! Computing reactant mixture specific heat
! Ref: Hill, P. G., and Peterson, C. R., Mechanics and
! Thermodynamics of Propulsion, 2nd ed., Addison-Wesley Publishing
! Company, 1992, Chap. 2.
CPMIX = 0
  DO 11 J = 1,NR
    CPMIX = CPMIX + (MF(J)*CP(J))
11 CONTINUE
CPMIX = CPMIX/MWMIX

R = RU/MWMIX ! Specific gas constant (J/kg-K)
GAMMA = CPMIX/(CPMIX-R)! Heat capacity ratio

! Computing inlet velocity and density of reactant mixture
CS1 = SQRT(GAMMA*R*T1) ! (m/s)
V1 = CS1*M1 ! (m/s)
RHO1= (P1/(R*T1)) ! (kg/m^3)

CALL EFFECTIVEGAS(RHO1,RHOE1,GAMMA,GAMMAE,CPMIX,CPE,CS1,CS1E,
M1,V1,V1E,R,RE,VOLFRAC)
! Emissivity of products of combustion is computed based on the work of Coppalle et al.
! Ref: Coppalle, A.,Vervisch, P., "The Total Emissivities of High-Temperature Flames,"
! Combustion and Flame, Vol. 49, 1983, pp.101-103.
! Computing partial pressures of CO2 and H2O in atm
PPCDX = FINXS(6)*PTOT
PPWAT = FINXS(5)*PTOT
PPRATIO = PPWAT/PPCDX
```

```
 ! Computing pressure path length product for emissivity calculation
PL = ((PPWAT + PPCDX)*L)! (atm-m)
! Modification made underneath in the if-else statement for partial-pressure
! Ratio to implement the selected emissivity model.
IF (PPRATIO.LE.1.5) THEN
   PPRATIO = 1.0
ELSE
   PPRATIO = 2.0
ENDIF
! Selection of emissivity coefficients based on modified partial-pressure ratio
IF (PPRATIO.EQ.1.0) THEN
  KI(1)=0.0D+00
  KI(2)=0.464D+00
  KI(3)=3.47D+00
  KI(4)=121.6D+00

  IF(TF.LT.2500) THEN
     ALPHA(1)= 0.0D+00
     ALPHA(2)= 0.136D+00
     ALPHA(3)= 0.516D+00
     ALPHA(4)= 0.0517D+00

     BETA(1)= 0.0D+00
     BETA(2)= 0.0000726D+00
     BETA(3)= -0.000163D+00
     BETA(4)= -0.0000176D+00

  ELSE
     ALPHA(1)= 0.0D+00
     ALPHA(2)= 0.464D+00
     ALPHA(3)= 0.336D+00
     ALPHA(4)= 0.0245D+00

     BETA(1)= 0.0D+00
```

```
      BETA(2)= -0.0000596D+00
      BETA(3)= -0.0000909D+00
      BETA(4)= -0.00000654D+00
    ENDIF
  ENDIF

  IF (PPRATIO.EQ.2.0) THEN
    KI(1)=0.0D+00
    KI(2)=0.527D+00
    KI(3)=3.78D+00
    KI(4)=99.54D+00

    IF(TF.LT.2500) THEN
      ALPHA(1)= 0.0D+00
      ALPHA(2)= 0.132D+00
      ALPHA(3)= 0.547D+00
      ALPHA(4)= 0.0489D+00

      BETA(1)= 0.0D+00
      BETA(2)= 0.0000725D+00
      BETA(3)= -0.000171D+00
      BETA(4)= -0.0000176D+00

    ELSE
      ALPHA(1)= 0.0D+00
      ALPHA(2)= 0.430D+00
      ALPHA(3)= 0.37D+00
      ALPHA(4)= 0.0184D+00

      BETA(1)= 0.0D+00
      BETA(2)= -0.0000472D+00
      BETA(3)= -0.000101D+00
      BETA(4)= -0.00000511D+00
    ENDIF
```

```
 ENDIF

EPSTOT = 0.0D+00
  DO 17 G = 1,4
  EPSTOT = EPSTOT + ((ALPHA(G)+(BETA(G)*TF))*(1-(EXP(-(KI(G)*PL)))))
17 CONTINUE
! Computation of emissivity ends

! Compute radiative heat flux
SIGMA = 5.67D-08 !Stefan–Boltzmann constant(W/(m^2 K^4))
QR = SIGMA*EPSTOT*(TF**4.0D+00) ! (W/m^2)

! Compute stagnation temperatures at entrance location (T01) & at
! exit location (T02), and Mach no. at exit location (M2) using model of a
! frictionless constant area flow with stagnation temperature change
! Ref: Hill, P. G., and Peterson, C. R., Mechanics and Thermodynamics
! of Propulsion, 2nd ed.,Addison-Wesley Publishing Company,1992,Chap.3.
T01 = T1*(1.0D+00 + ((GAMMA - 1.0D+00)/(2.0D+00))*(M1**2.0D+00)) !(K)
DELTAT0=(QR/(RHO1*V1*CPMIX))
T02=T01 + DELTAT0 ! (K)
KK2 = T02/T01
CC1 = (((1+(GAMMA*(M1**2.0D+00)))/M1)**2.0D+00)
CC2 =  (1/(1+(((GAMMA-1.0D+00)/2.0D+00)*(M1**2.0D+00))))
KK1 =  CC1*CC2
KK=KK2/KK1
P01 = P1*((1.0D+00 + ((GAMMA -
1.0D+00)/(2.0D+00))*(M1**2.0D+00))**(GAMMA/(GAMMA-1))) ! Stagnation pressure at
entrance location(Pa)
 AK = ((KK*(GAMMA**2.0))-((GAMMA-1)/2))
BK = ((2.0*GAMMA*KK)-1.00)
DK = 1- (2*KK*GAMMA) - (2*KK)
MS1 = (- BK + (SQRT(DK)))/(2*AK)
MS2 = (- BK - (SQRT(DK)))/(2*AK)
M2 = SQRT(MS1)
```

```
T2=T02/(1.0D+00 + ((GAMMA - 1.0D+00)/(2.0D+00))*(M2**2.0D+00)) ! (K)
P2 = ((P1*M1)/M2)*((T2/T1)**0.5D+00) ! (Pa)

! Solving of finite difference formulation using model of a frictionless constant area flow
! with stagnation temperature change- it provides flow properties for the upstream region
! Ref: Hill, P. G., and Peterson, C. R., Mechanics and Thermodynamics of Propulsion, 2nd
! ed., Addison-Wesley Publishing Company, 1992, Chap.3.
! Initializing at I=1
I=1
T0(I)=T02
Q(I)=QR
M(I)=M2
T(I)=T2
P(I)=P2
C(I)= SQRT(GAMMA*R*T(I))
U(I)=C(I)*M(I)
RHO(I)= (P(I)/(R*T(I)))
P0(I) = P(I)*((1+((GAMMA-1)/2)*(M(I)**2))**(GAMMA/(GAMMA-1)))
QT = (QR/(RHO(I)*U(I)))     !J/kg

TOL = ((0.1/100)*QT)

QSUM = 0.0
DO 12 I = 1,1999999
SELECT CASE (FUEL)

  CASE (1)
  ! Absorptance of ethane is obtained from work of Olson et al.
  ! Ref:Olson, D. B., Mallard, W. G., and Gardiner, J. W. C., "High
  ! Temperature Absorption of the 3.39 μm He-Ne Laser Line by Small Hydrocarbons,"
  ! Applied Spectroscopy, Vol. 32, No. 5, 1978, pp. 489-493.
  ABSORPTIVITY(I) = 48100-(10.01*T(I))-(0.0017*(T(I)**2.0D+00)) ! (cm^2/mol)
  OPTPATH = 0.005  !(cm)
  CONC(I)= (6.8078D-09)*(P(I)/T(I)) ! (mol/cm^3)
```

```
   ABSORPTANCEC(I)= (ABSORPTIVITY(I)*OPTPATH*CONC(I))

   CASE (2)
  !Absorptance of methane (case 2) and syngas (case 3) is obtained from work of Wakatsuki,K.
   !Ref:Wakatsuki, K., "High Temperature Radiation Absorption of Fuel Molecules And
   !An Evaluation of Its Influence on Pool Fire Modeling",Ph.D. Dissertation,
   !Department of Mechanical Engineering,University of Maryland,College Park,MD,2005.
   KP(I) = (-1.8267D-05)+((3.9617D-07)*T(I))+((-7.7619D-
   10)*(T(I)**2.0D+00))+((5.7857D-13)*(T(I)**3.0D+00))+((-1.5283D-
   16)*(T(I)**4.0D+00))!(1/(m-Pa))
   ABSORPTANCEC(I)= (0.00005*P(I)*KP(I))

   CASE (3)
   KP(I) = (-1.8267D-05)+((3.9617D-07)*T(I))+((-7.7619D-
   10)*(T(I)**2.0D+00))+((5.7857D-13)*(T(I)**3.0D+00))+((-1.5283D-
   16)*(T(I)**4.0D+00))
   ABSORPTANCEC(I)= (0.00005*P(I)*KP(I))

 END SELECT

!Absorptance of carbon particles is obtained from the work of Modest.
!Ref: Modest, M. F., Radiative Heat Transfer, 3rd ed., Elsevier Science and
!Technology Books, Chap. 12.
 ABSORPTANCED = 0.01674*(10**6)*VOLFRAC*0.005

!Combined absorptance of gas-solid mixture is obtained from the work of
!Viskanta et al.
!Viskanta, R., and Menguc, M. P., "Radiation heat transfer in combustion systems,"
!Progress in energy and combustion science, Vol. 13, 1987, pp. 97-160.
 ABSORPTANCE(I) = ABSORPTANCED + ABSORPTANCEC(I)

WRITE (20,*) -(I-1)*0.00005, ABSORPTANCED ,  ABSORPTANCEC(I),
 ABSORPTANCE(I)
T0(I+1) = T0(I) - ((ABSORPTANCE(I)*Q(I))/(U(I)*RHO(I)*CPMIX))
```

```
QABSD(I) = (ABSORPTANCE(I)*Q(I))/(RHO(I)*U(I))
QSUM = QSUM + QABSD(I)
Q(I+1) = Q(I)-(ABSORPTANCE(I)*Q(I))
ERROR = QT - QSUM
IF (ERROR.LE.TOL) GOTO 40
K2=T0(I+1)/T0(I)
C1 = (((1+(GAMMA*(M(I)**2.0D+00)))/M(I))**2.0D+00)
C2 =  (1/(1+(((GAMMA-1.0D+00)/2.0D+00)*(M(I)**2.0D+00))))
K1 =  C1*C2
K=K2/K1
A = ((K*(GAMMA**2.0))-((GAMMA-1)/2))
B = ((2.0*GAMMA*K)-1.00)
D = 1- (2*K*GAMMA) - (2*K)
MSQ1(I+1) = (- B + (SQRT(D)))/(2*A)
MSQ2(I+1) = (- B - (SQRT(D)))/(2*A)
M(I+1)= SQRT(MSQ1(I+1))
T(I+1) = (T0(I+1))/(1.0D+00 + ((GAMMA - 1.0D+00)/(2.0D+00))*(M(I+1)**2.0D+00))
C(I+1) = SQRT(GAMMA*R*T(I+1))
U(I+1) = (M(I+1)*C(I+1))
RHO(I+1) = (RHO(I)*U(I))/U(I+1)
P(I+1) =   RHO(I+1)*R*T(I+1)
P0(I+1) = P(I+1)*((1+((GAMMA-1)/2)*(M(I+1)**2))**(GAMMA/(GAMMA-1)))
12 CONTINUE

40 N = I

WRITE (19,*) 'VARIABLES = "X", "Q"'
WRITE (16,*) 'VARIABLES = "X", "T"'

DO 13 I= N,1,-1
! Writing flow variables in their respective files
WRITE (16,*) -(I-1)*0.00005,  T(I)
WRITE (17,*) T0(I)
WRITE (18,*) P0(I)
```

```
WRITE (19,*) -(I-1)*0.00005,  Q(I)
WRITE (8,*) -(I-1)*0.00005
WRITE (9,*) P(I)
WRITE (10,*) M(I)
WRITE (11,*) (RHO(I)*U(I))

13 CONTINUE

RETURN
END

SUBROUTINE
 EFFECTIVEGAS(RHOC,RHOE1,GAMMAC,GAMMAE,CPC,CPE,CS1,CS1E,M1,V1C,V1
 E, RC, RE, ALPHAD)
!Subroutine 'EFFECTIVEGAS' is used to account for solid phase properties and
!to treat the gas-solid mixture as a single phase gas or an 'effective gas'
DOUBLE PRECISION ALPHAC, ALPHAD, CSD, CVC, EPSILON, RHOD,
 RHOC,RHOE1,GAMMAC
DOUBLE PRECISION GAMMAE,CPC,CPE,CS1E,V1E,V1C, RE,RC, CS1, M1
!---------------------------------------------------------------------
! Variables
! RHOC = Density of continous (gaseous) phase  (kg/m^3)
! RHOE1 = Density of effective gas  (kg/m^3)
! GAMMAC = Heat capacity ratio of continous phase
! GAMMAE = Heat capacity ratio of effective gas
! PTOT = Total pressure of gases in the downstream region (atm)
! CPC = Specific heat capacity of continous phase (kJ/kg-K)
! CPE = Specific heat capacity of effective gas (kJ/kg-K)
! CS1 = Speed of sound in continous phase (m/s)
! CS1E = Speed of sound in effective gas (m/s)
! M1 = Mach number
! V1C = Velocity in continous phase at entrance location (m/s)
! V1E = Velocity in effective gas at entrance location (m/s)
! RC = Specific gas constant in continous phase(J/kg-K)
```

```
! RE = Specific gas constant in effective gas (J/kg-K)
! ALPHAD = Volume fraction of carbon particles (disperse phase)
!-----------------------------------------------------------------------
!Formulation is based on the work of Brennen, C.E.
 !Ref: Brennen,C. E.,Fundamentals of Multiphase Flows,Cambridge University
 Press,2005,Chap. 11.
ALPHAC = 1-ALPHAD
CSD = 710.0D+00 ! Specific heat of carbon particles(kJ/kg-K)
CVC = CPC/GAMMAC
RHOD = (2267.0D+00) ! (kg/m^3)
EPSILON = ((RHOD*ALPHAD)/(RHOC*ALPHAC))
RHOE1 = RHOC*(1+EPSILON)
GAMMAE = ((CPC + (EPSILON*CSD))/(CVC + (EPSILON*CSD)))
CPE = ((CPC + (EPSILON*CSD))/(1 + EPSILON))
CS1E = CS1*(SQRT((1 + ((EPSILON*CSD)/CPC))/((1 + ((EPSILON*CSD)/CVC))*(1 +
 EPSILON))))
V1E = M1*CS1E
RE = (RC/(1 + EPSILON))
RHOC = RHOE1
GAMMAC = GAMMAE
CPC = CPE
CS1 = CS1E
V1C = V1E
RC = RE
RETURN
END
```

VITA

Shubhadeep Banik was born in Tinsukia, India. He completed schooling from Kolkata, India in 2007. Thereafter, he enrolled in an undergraduate program in Mechanical Engineering in the National Institute of Technology Durgapur, India. He obtained a Bachelor of Technology degree in Mechanical Engineering in September 2011. To further his education, he chose a masters program in Mechanical Engineering at the Missouri University of Science and Technology, Rolla, Missouri, USA. In May 2015, he received his Master of Science degree in Mechanical Engineering.